Hugo Miguel Mantas Costa Pinto

Licenciatura em Engenharia Eletrotécnica e de computadores

Robotic Exoskeleton Hand with Pneumatic Actuators

Dissertação para obtenção do Grau de Mestre em
Engenharia Eletrotécnica e de Computadores

Orientador: Doutor José Barata de Oliveira, Professor Auxiliar, FCT-UNL

Júri:

Presidente:	Prof. Maria Helena Silva Fino
Arguentes:	Prof. João Almeida das Rosas
Vogais:	Prof. José António Barata de Oliveira

FACULDADE DE CIÊNCIAS E TECNOLOGIA
UNIVERSIDADE NOVA DE LISBOA

Outubro, 2016

Robotic Exoskeleton Hand with Pneumatic Actuators

"The first step is to establish that something is possible; then probability will occur."

Elon Musk

Acknowledgements

I would first like to thank my thesis advisor Doctor Jose Barata of the Faculty Science and Technology at Nova Lisbon University. The door to Prof. Barata office was always open whenever I ran into a trouble spot or had a question about my research or writing. He consistently allowed this paper to be my own work, but steered me in the right the direction whenever he thought I needed it.

I would also like to thank the experts at RICS who were involved in the validation survey for this research project: Francisco Marques – PhD Student, Ricardo Mendonça – PhD Student, André Lourenço – PhD Student, Eduardo Pinto – PhD, Carlos Simões – PhD, Lino Quaresma – EngTech. Without their passionate participation and input, the development of this device could not have been successfully conducted.

Finally, I must express my very profound gratitude to my family and friends for providing me with unfailing support and continuous encouragement throughout my years of study and through the process of researching and writing this thesis. This accomplishment would not have been possible without them. Thank you.

Resumo

Com o moderno desenvolvimento de dispositivos inteligentes moveis e com a miniaturização da tecnologia, a sociedade tem sido dotada de assistência computacional para quase todas as atividades diárias, mas os aspetos físicos são frequentemente esquecidos. Já é possível construir robôs que processam informação através de redes neuronais, que exprimem e identificam expressões emocionais e que substituem o trabalho manual nas fábricas, aproximando-se cada vez mais das capacidades associadas ao ser humano. Apesar de estes sistemas serem mantidos próximos continuam separados do ser humano, substituindo-o ou executando outros serviços de suporte não sendo geralmente adotada a vertente de apoio simbiótico físico e direto do utilizador.

Nesta dissertação será descrita uma mão exosqueleto robótica que permite interação bidirecional homem-máquina tornando possível a assistência eletromecânica em diversos tipos de atividades físicas. Este sistema é desenhado de modo a imitar as funcionalidades e estrutura biomecânica da mão humana, incluindo mecanismos sensoriais e de controlo.

Para validação do conceito apresentado foi construído um protótipo parcial utilizando componentes facilmente adquiridos no mercado.

Palavras-chave: exosqueleto, prótese, mão robótica.

Abstract

With modern developments of smart portable devices and miniaturization of technologies, society has been provided with computerized assistance for almost every daily activity but the physical aspects have been frequently neglected. It is currently possible to make robots that process information thru neural networks, that identify and mimic facial expressions and that replace manual labour in assembly plants, getting ever closer to skills associated to human beings. In spite of these technological advances being kept close to they remain separate of humans, replacing or providing assistance with other peripheral tasks, not generally adopting a direct physical symbiotic user assistance path.

In this dissertation a robotic exoskeleton hand will be described that allows for human-machine bidirectional interaction making it possible to provide physical activities with the electromechanical assistance similarly. This system is designed to mimic the human hands functionalities and biomechanical structure, as well sensing and controlling systems.

A partial prototype was also built, using components easily acquired in the market, as a proof of concept.

Keywords: Exoskeleton, prosthetics, robotic hand.

Content

List of Figures

1

Introduction

Motivation

Exoskeletons are a type of skeletal architecture that surrounds the wearer instead of the traditional internal design. Exoskeleton wearable robots follow the same principle of having the pivotal structures outside its user allowing the mechanical system to be used as a suit.

This type of robotics allows an intuitive and natural interaction between human and machine where the users are not required to steer nor actively control the robot but instead have only to move their body while the exoskeleton follows.

Exoskeleton structures are a common tool for therapy where they are able to restrict the wearer to the correct movements their body is supposed to execute. This prevents further damage to the patients' body while allowing the medical professional to perform the prescribed exercises, or returning some of the mobility lost due to injury or disease.

Similar exoskeleton structures can be used as input devices for easy human control of separate mechanisms, as is being applied in surgical procedures allowing the remote control of specialized equipment, and in virtual environment interaction where the user can interact with objects rendered inside of digital devices.

A less developed application of these systems is in human augmentation and is being researched by military, medical, industrial and academic organizations with the objective of bringing the best from mechanical and biological sys-

tems together by complementing each other expanding their functionalities beyond each of their limitations.

In this dissertation it is presented an exoskeleton hand able to mimic its biological equivalent in dexterity and flexibility reducing the limitations of previous systems and reducing the volume and mechanical interference commonly associated with such devices.

Objectives

The main objective of this dissertation is to design an exoskeleton glove capable of performing the same range of movements the human hand is able to while making the joint structure self-supportive adding independent robotic capability to the device.

To achieve the set objectives several stages were identified:

- Conceive a finger joint mechanism capable of performing both rotation and translation from the outside of the finger with reduced height and rigid movement path;
- Design an ergonomic structure to support the actuators, sensors and controller coupled with the actuated hand;
- Build and test artificial pneumatic muscles in order to gather data on the actuators performance;
- Plan a control system to process sensory information from strain gauge in to actuator commands.
- Construct a prototype of the finger joint with sensors and actuators to validate the system design.

The base requirements of the project are:

- Have the same number of degrees of freedom observed in the biological hand;
- Self-contained system;
- Invisible control approach;
- Fast and strong movement, comparable to human hand.

Dissertation Structure

The dissertation is divided into six chapters which, with the exception of this introductory one, are:

- ⇒ **Chapter 2: State of the Art** Analyses of the developments made in the area of exoskeleton gloves and the different approaches to each mechanical, electrical and complexity problems;
- ⇒ **Chapter 3: Supporting Concepts** Study of the biological system the exoskeleton intends to mimic and comparison of the structural and mechanical properties used in the artificial design in relation to their organic equivalent;
- ⇒ **Chapter 4: Mechanical Architecture** Description of the design and calculations of the mechanical and physical structures developed for this project;
- ⇒ **Chapter 5 Actuation** Measurements and experimental data analysis of the built pneumatic muscles and their respective valves and supply system;
- ⇒ **Chapter 6: Control** Development of the control and data gathering circuit and the relevant microcontroller programing and controller design.

2

State of the Art

2.1 - Common objective of existing exoskeleton devices

Exoskeleton hands have been and are being developed with different objectives to be applied in distinct areas like rehabilitation, human augmentation, remote manipulation or interaction in virtual environments.

2.1.1 - Rehabilitation or therapy

Most exoskeleton hands structures are designed to help doctors perform rehabilitation exercises on patients that had a stroke or suffered from tendons or muscle injuries while, in some cases (as in [1]–[3]), allowing them to measure and record the movements and forces exerted by the patient which will help to better diagnose the condition of the injury and improve the therapeutic exercises and specifications.

This type of exoskeleton tend to work exclusively in slave mode where the equipment used by the patient receives commands from a computer, with a treatment plan specific for the individual patient and the device being used, or by being remotely controlled by the doctor in real time. On some cases, the user can move the robotic glove by himself, with the aid of a controller glove or using EMG signals collected on different muscles that do not interfere with the hand being treated.

Devices used for this purpose tend to cover less fingers or less independence between them instead focusing on slow and precise movements of each

articulation to reduce the discomfort for the patient and correct the disability they were designed to help repair.

2.1.2 - Augmentation

Surpassing the human limitations using robotic devices to augment strength or stamina (as in [4], [5]) is an objective that would be beneficial for both private and corporate sectors. Exoskeleton hands have been developed for this purpose but haven't yet been implemented, possibly due to the high cost of the device or the lack of positive feedback from this technology, caused by this technology novelty.

Increasing workers stamina would improve productivity in repetitive or straining tasks while increased strength could reduce the need of other less versatile mechanical equipment. Other augmentation that exoskeleton systems allow is the addition of functionalities not available in the original biological structure (as in [6]).

2.1.3 - Telemanipulation

When humans are unable to, or put in danger if, interact directly with objects there is a need to replace the human factor for a mechanical system. This is usually done with specific equipment that although work very well in regular circumstances have very limited versatility, leaving the operation susceptible to unexpected circumstances, and may not be particularly intuitive to operate, requiring extensive training and being prone to operating mistakes.

By applying human-like manipulation to the mechanical gripers and controlling those with exoskeleton master system (as in [7]) it has been made possible to remotely interact with delicate or dangerous objects with similar dexterity to that of the human operators while keeping them a safe distance away or outside restricted areas.

Replacing the human hands with robotic counterparts can also improve the interaction with the environment, for instance, when a smaller mechanism than the human hand is required. An example of this is how it is being done in chirurgical operations where the doctor manipulates small robotic gripers that enable him to perform procedures in a safer and less intrusive way.

2.1.4 - Virtual Manipulation

One of the easiest ways to interact with a virtual environment is to grab the virtual objects as if they were in the physical world with the help of exoskeleton sensory gloves. These devices transmit the finger movements, detected thru sensor arrays, to the computer, while most times also providing force feedback (as in [8]) which effectively gives the user the ability to touch virtual objects has if they were real.

This type of computer interaction is very useful for computer design of 3D objects and structures, allowing the designer to observe their design in different perspectives and more easily sculpt their creation, or for product designers to interact with the virtual prototype without having to have it manufactured allowing them to confirm that it follows the desired specifications and, if needed, improve ergonomics.

Other additional functionalities made available by this type of devices are easy hand gesture identification so that they can be interpreted by the computer, acting as a joystick, a keyboard or a pointer all in one for a versatile interface system (as in [6]).

2.2 - Degrees Of Freedom

In order to reduce the complexity of the system and the number of actuators required, it is common to couple joints to a single actuator reducing the number of degrees of freedom and limiting the dexterity of the exoskeleton hand.

By carefully selecting which joint to couple and how to distribute the force of the actuator (as in [2], [4]) the objective for the project may still be reached with reduced costs, lighter overall device weight and lower power consumption.

However, this practice limits the functional flexibility of the equipment, and with it, the marketability of the device and the potential interest in its improvement making it necessary to develop several different systems for each functionality.

2.3 - *Joint Mechanism*

In an exoskeleton, the joint mechanism implemented has to be able to perform an identical movement to that of the structure it is intended to follow or mimic.

To do that, there are almost as many methods as there are devices that apply them but they can be divided by the two basic considerations taken when selecting which one to implement. If the external joint is placed in line with the centre of rotation, for example in the case of the finger, it would be placed laterally. Alternatively it may have a remote centre of motion, requiring rotation and translation simultaneously to perform the same movement instead of exclusively rotation as in the previous style.

2.3.1 - Four-bar mechanism

An inverted "V" shaped structure that, when the top pulley is pulled down, opens the joint and can be closed by pulling the two bases together (as illustrated in Fig. 2.1). By adjusting the pulley diameter it is possible to rotate the bar connecting the mechanism to the farthest base to accompany the movement of the users finger but it is not very reliable due to slipping of the cables over the pulleys leading to devices using this mechanism to always require an internal skeletal model, either an users hand or a prosthetic substitute.

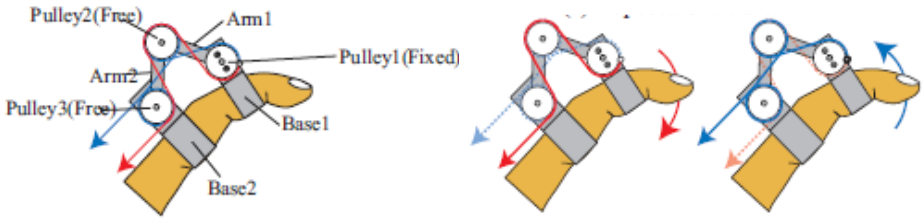

Fig 2.1: An example of the four-bar mechanism used to transmit power to the phalanges (Taken from [1])

2.3.2 - Five-bar mechanism

The five-bar mechanism works quite differently from the previously mentioned four-bar mechanism in that it has five rotating points (as shown in Fig. 2.2) instead of the aforementioned tree, this makes it possible to transfer the force used to close one joint to the following ones allowing the finger to apply

identical force thru all of its length without cables passing thru all the pulleys of each finger joint.

This technique, although beneficial for reducing actuation complexity, also eliminates the possibility of adding more degrees of freedom to an individual finger due to the structure requiring the mechanical linkage to create the rotating motion.

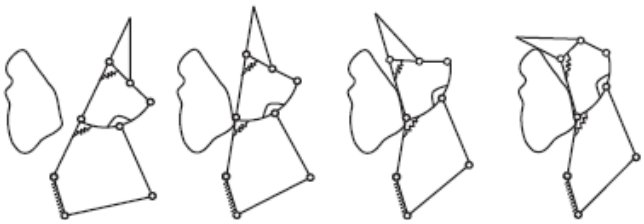

Fig 2.2: Schematic exemplification of the motion from a five-bar mechanism against an object (Taken from [2])

2.3.3 - Six-bar mechanism

Unlike the previous two approaches to external joint movement, this six-bar mechanism is able to produce rotation and translation independently of an internal skeleton making it possible to move autonomously like a robotic hand. Another difference with previously described mechanisms is that the rigidity of the rotation gives it a fixed remote centre of rotation (as represented in Fig. 2.3) meaning that it cannot be implicitly adapted to different length fingers.

This system works in a similar fashion to a scissor mechanism where the width between the bases gets longer as the height of the structure gets shorter. The difference is that the interconnectivity between the two bases and two extra bars adds rotation to the bases mimicking the rotation and translation of the users' fingers articulation.

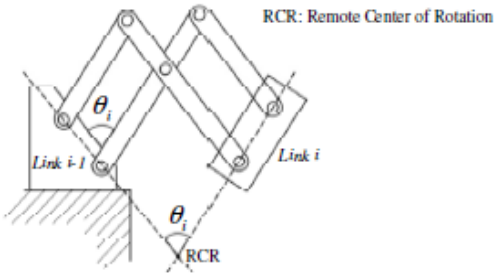

Fig 2.3: Scheme depicting the remote centre of rotation in a six-bar mechanism (Taken from [8])

2.3.4 - Circuitous joint

This joint mechanism uses a combination of gears rolling over racks (as shown in Fig. 2.4) that add rotation to the moving part as it slides outwards resulting in rotation and translation of the joined sections that mimic the fingers movement.

With the repulsion force exerted by a compression spring pushing on the centre of the gears axis the mechanism flexes, returning to the linear position when a cable pulls on the outer section. The system is stable and rigid, allowing it to move independently from an internal structure but it is also not adjustable to different sized hands and the spring limits the grasping dynamic to a specific maximum performance, because the force and speed of the springs' extension cannot be altered.

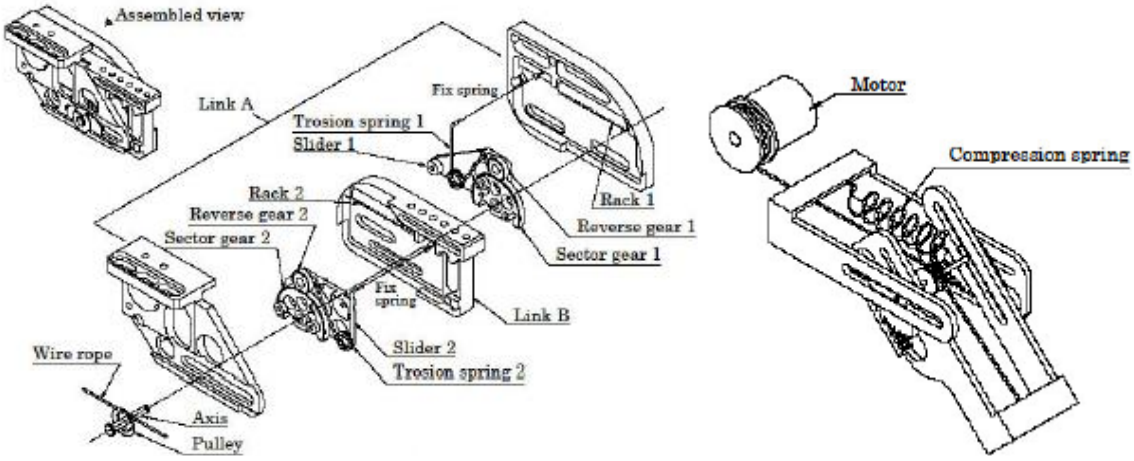

Fig 2.4: Schematic of a circuitous joint mechanism with sliders and spring (Taken from [7])

2.3.5 - Revolute joint

Pining both sides of a moving joint together concentrically (as shown in Fig. 2.5) to the rotation centre is the simplest method to make sure the movement will be executed along the expected path in a rigid and reliable way while allowing the movement to be actuated around the pivot with a plain pull or push of the dependent side.

Advantages of this system is the independence from internal skeletons or guiding structures, giving the device a robotic functionality separated from an internal skeleton, and the simple and direct force exertion on the moving part but when applied to the interphalangeal of the users fingers it adds thickness making it uncomfortable, and maybe even dangerous, during continuous use.

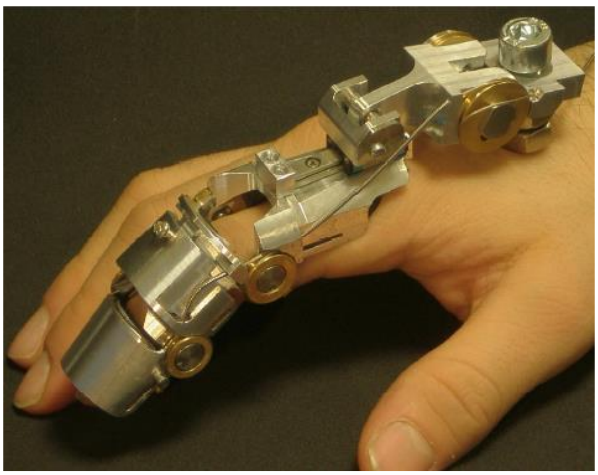

Fig 2.5: Example of a finger exo-skeleton with a revolute joint on the interphalangeals and a Slider-crank mechanism on the metacarpophalangeal (Taken from [3])

2.3.6 - Slider-crank mechanism

Combining a revolute joint with a longitudinal sliding base results in a mechanism that can slide from the original position of an extended finger to the length of its flexed position with the revolute section providing the angular component of the movement (as shown in Fig. 2.5).

Being a solution for the translation problem, occurring in outer path of the human fingers flexing motion, similar to the circuitous joint but without the gears to keep the motion regular makes this a less reliable approach to the issue but the sliding mechanism allows for self-adjusting finger length that was not possible in some of the previously described joints.

2.3.7 - Trapezoidal linked lever

A trapezoidal mechanism (as shown in Fig. 2.6) is similar to the five-bar mechanism in design and use but with less mechanical parts. This system is able to apply force to the outside of the entire finger thru progressively lower levers that redirect the energy toward the closing movement of each finger section with a balanced distribution of pressure.

Closing speed and priority of each rotation point is not directly imposed reducing the repeatability of the same movement and making this a less than reliable mechanism when being used as robotic hand.

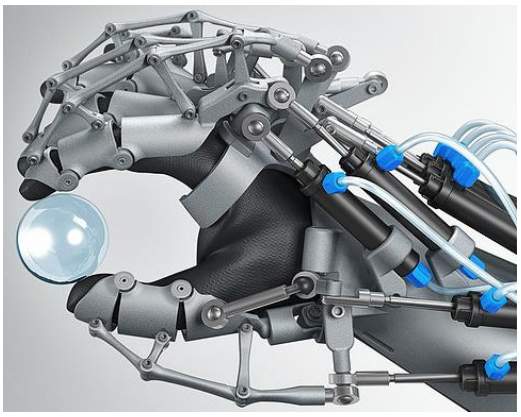

Fig 2.6: Picture of the Festo Exohand that uses a trapezoidal linked system to distribute force to the phalanges (Taken from [9])

2.4 - Independent Stability

The structure selected for the joint mechanism can impact the available functions of the exoskeleton. If the articulation between the moving parts of the glove is able to reliably and repeatedly reproduce the human motion without an internal skeletal structure to guide the movement (as in [8]) and the length of each section can be locked or is fixed then the exoskeleton mechanism is able to act as a robotic hand. This makes it possible to use the same device for tele-manipulation without having to calculate the corresponding action for the movement detected in the master glove.

2.5 - Operation Classification

An Exoskeleton systems operation can be divided in to two generic classifications, it can either be a controller or a master, which detects commands from a user and transmits them to a receptive device, or it can be a slave system that receives commands from an external device and operates according to the instructions acquired. Most devices, to some extent, combine parts of each of these operation classes by having the controller collect data from the slave to transmit to the user as feedback or by having both the sensors and actuators in to a single device making it able to move itself according to data collected by sensors in the actual mechanism.

2.5.1 - Controller

An exoskeleton glove is a convenient way to provide ergonomic computer interface to a human user as it detects the movement from a body part that is very dextrous as well as being regularly, and unconsciously, used in interpersonal communication.

Exoskeleton master gloves (as in [8]) are covered with sensors to detect a variety of data ranging from movements to pressures and forces that can be decoded and interpreted by processing unit and transmitted to the virtual environment simulator or slave robotic device.

The movement of sensor gloves is sometimes restricted by feedback actuators that limits the users' movements according to the resistance the slave device encounters, this is very useful specially when manipulating objects in virtual environments, by adding one more sensory input to the user.

2.5.2 - Slave

When a robotic system follows instructions given by a second device the first one is classified as a "slave" and some exoskeleton gloves (like in [3]) work in this manner, where the movement imposed by the actuators is controlled by instructions on a computer or from a secondary device, like a different exoskeleton glove or a separate sensor like EMG or brainwave reader.

The use of this configuration is common in therapeutic applications where the medical practitioner instructs the mechanical device to move in a particular manner in accordance to the prescribed exercises appropriate for the patients' condition.

2.5.3 - Exo Follow Hand

Combining the previous two operation classifications results in an exoskeleton capable to follow the human hand (as in [4]), making it invisible while wearing, or to even help with the users activities, augmenting force or stamina (as in [5]).

Devices that can follow a users' movement can also be used instead of each of the previous ones, not being limited by hardware, making them a more versatile choice.

2.6 - Digit Coverage

Exoskeleton gloves are a compilation of independent actuators, sensors and moving structures that add a lot of complexity, weight and cost to the device, that is why it is common practice to limit the systems digit coverage to the

necessary number of digits or make them modular to allow for users to adjust the configurations according to their needs.

In therapeutic and medical applications, the focus is on individual fingers and here is where there are more examples of modular (as in [3]) or coupled finger mechanism. This is an advantage for both the patient and the physician because the first has to endure less discomfort from having this equipment imposing exercises on damaged or injured parts and for the doctor for it allows him to precisely apply treatments without interfering with adjacent digits.

For telemanipulation and virtual manipulation, the usual approach is to only include in the exoskeleton glove the index and thumb (as in [8]). This allows controlled mechanism or simulation to act as a claw, grasping objects with sufficient precision without cluttering the processing unit with extraneous signals from the remaining fingers.

When the purpose of the exoskeleton is to improve on human limitations or more dexterity is needed a full hand is designed (as in [4]), but even in this situation some concessions are granted. Due to the importance of the index and thumb for the grasping motion these two are always included but the remaining fingers may be coupled or given less degrees of freedom. It is possible to find examples of coupling of the ring and little finger to a single sensor or actuator or even to have the little finger not included in the project. Due to the limited utility of the last finger it is understandable that, to reduce overall complexity and weight, this digit is coupled with the adjacent one or simply not included.

2.7 - Speed

Finding a balance between precision and speed is hard when the system has no way of knowing the amplitude of the desired movement. If we consider in addition to this the signal filtering, required to eliminate noise associated with the irregular circumstances the sensors are operating in, and the delay associated with the operation of the actuators, the result is a slowed reaction speed that will reduce the precision of the movement in fast and short actions.

This problem is amplified with several designed factors like the mechanical movement transmission method and static attrition of the joints that add an oscillating response to the force applied by the actuators. This may be imper-

ceptible to the human eye but it adds to the noise of the sensor and interferes with the movement of the human finger.

Most exoskeleton devices developed are meant to be used in average or slow hand movements avoiding problems associated with the mechanical limitations of fast impulses.

2.8 - Force

Grasping force is a parameter that is often put in to the compromise section to be reduced in exchange for lighter mechanism and more precise movement. This relation between power and weight results from the predominant use of electric actuators that to provide more power have to be bulkier than other equally efficient but less powerful models.

Some exoskeletons use a different actuation type that relies on energy sources that are not electric (as in [10]), still requiring electric energy to control the device. This systems can outperform the human hand but are less precise and, depending on many factors, for the most part are slower than the electric actuators.

2.9 - Autonomy

Autonomy is a problem affecting many electronic devices, mainly due to the low energy density in current batteries. This is more pronounced on equipment that require more powerful actions for example when an exoskeleton device tries to match or surpass the human mechanical strength. Due to this, and the fact that with increased number or volume of batteries, the global weight of the device also increases, making it harder to transport, most exoskeleton gloves opt for stationary power supply, and since it is going to be grounded they move the controller, and sometimes the actuators, to an external station as well.

This compromise reduces the usefulness of such technology limiting them to labs, factories and offices. Mobile operations are possible with external supply systems which keeps the mechanism stationary and merely move the stations location.

The alternative being applied to add mobility to the exoskeleton mechanisms is to make them less powerful and less dextrous reducing the power requirements and the active time of the device making it able to be easily carried and used (as shown in Fig 2.7).

Fig 2.7: Example of an exoskeleton glove with actuators controllers and power systems incorporated in to the glove (Taken from [11])

2.10 - System Control methods

Controlling an exoskeleton glove depends on several mechanical and conceptual factors but the first differentiation on which approach to take is if the glove will be working in a master or slave configuration, or both shadowing the user.

For a slave type controller the system must be able to move to the same position, or apply the same pressure, instructed by the master and, when capable, respond with the sensory information of obstacles to the movement.

In a master glove, the objective of the controller is to detect the movement intended by the user and translate the adequate command to the slave system while keeping constant distance to the human finger or constant pressure on the fingertips. In case the exoskeleton hand has feedback capabilities the controller will have to be able to change detection methods, from position, when the slave system is free to move, to pressure sensing, to indicate how much force the motors must apply, and control its own actuators to mimic the resistive force felt by the slave device.

When the exoskeleton glove follows the users' movements directly the controller mixes the two controlling approaches into one and this, ironically, makes the control easier because the feedback capability is intrinsic to the mechanism reducing the number of sensors required as well as the mechanical actuations and the signal processing between the two.

2.11 - Difficulty of Use

For the most part, exoskeleton gloves are easy to use. They are either designed to sense the users' movements or to impose certain exercises regardless of the users will, but some have separate controls that are not intuitive, requiring some training and calibration.

Regardless of the control method, they all impose upon the wearer the sense that he is not simply moving his own body but that there is something else restricting his movements, in reaction speed or added weight, and sometimes improving on his limitations, for example improving strength and stamina. No exoskeleton developed outside of science fiction is completely invisible to the users' senses but many try to make its restrictions negligible, especially compared to the advantages it brings.

2.12 - Sensors

Almost all exoskeleton gloves requires sensors to work, even if those sensors are not on the device they will be connected to its controller and be used to either collect data for analyses, for medical purposes for example, or directly translated in to commands for movement actuation or remote manipulation, in either real or virtual environments.

2.12.1 - Pressure

Measuring the pressure exerted by the user on the sensor allows the system to adjust the power provided to the actuators, whether in the original system or the slave device.

This is the only sensor type that allows for the user to directly adjust the force the grasping device or the exoskeleton will exert on the object held, if the object is removed this sensor will lose the signal indicating for the actuators to stop the movement unlike the following sensors.

2.12.2 - Position

Many exoskeleton gloves with sensing capabilities have position sensors that change resistance according to the fingers position, detect the fingers distance to the sensor or that, when moved by the user, are able to calculate the amplitude of displacement that corresponds to that particular position.

Regular calibration is required for some of these sensors so continuous operation for long periods of time result in reduced precision and are dangerous if used alone because they may cause damage to the object they are holding or even to the glove itself by exerting excessive force to try to reach the desire position.

2.12.3 - EMG

Electromyography is used by some systems as an input technique that measures the electrical activity of the users' muscles (as shown in Fig. 2.8) and instructs the actuator to perform the task corresponding to that signal, those commands are assigned to each relevant electrical signal measurable.

Signal decomposition is difficult due to the uncertainty of the muscle position, the sensor is located on the skin surface and the muscles change their relative position with unrelated movements, and the fact that electrical impulses from deeper muscles interfere with those originated by surface muscles making the positioning and reliability of this type of sensors for robotic control an issue.

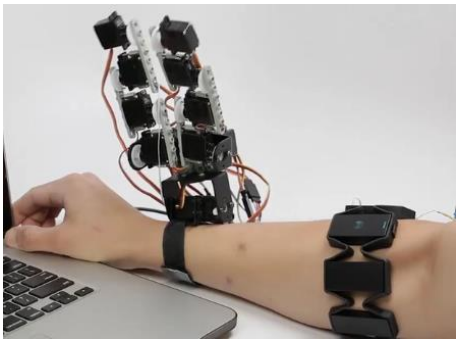

Fig 2.8: Example of an EMG sensor controlling two robotic fingers (Taken from [6])

2.12.4 - Brain-computer interface

By means of electroencephalography (EEG) the electromagnetic fields generated by electric communication between neurons can be detected and roughly identified (as exemplified in Fig. 2.9). With this type of sensor the user can instruct the actuators with the desired movement just by thinking it but it is very hard to distinguish signals from each other and it requires a lot of practice and concentration to be used properly.

This input method has the most potential but is still very limited, leading to systems with equally limited movements and a steep learning curve with the added disadvantage of being vulnerable to errors when external factors interfere with the users attention or with the established baseline.

Fig 2.9: Two examples of brain-computer interfaces (Taken from [12], [13])

2.13 - Critical analysis

Most of the systems developed so far have been purpose oriented, with functional limitations intended to improve the overall performance and reduce complexity and cost of the device.

By combining good examples from different implementations and designing new architectures to improve the performance of previous mechanism, it is possible to overcome the limitations of previous projects creating a more functional and multi purposed equipment.

To create an electromechanical system able to provide assistance, or remotely replace, the biological human hand in an efficient and symbiotic way many different disciplines have to be involved. For the study of the biomechanical structure and movement vectors the development team will require some anatomical knowledge. A mechanical and physical perspective will work in close proximity to the previous knowledge base to create an adequate artificial substitute structure, this has to be able to provide support in excess to what the original structure is capable of while allowing for an identical combinations of movements. The devices artificial nervous, cognitive and actuation functions will require electrotechnical expertise, for the sensory component and processing as well as for triggering actuation, regardless of the nature of the selected actuators.

Studying the human hand structure, which the exoskeleton mechanism is attempting to mimic, reveals multiple degrees of freedom in each finger, these finger and hand dexterity evolved due to the need humans had for them. Following that logic, the exoskeleton glove should be able to at the very least be

able to match the flexibility of the system it is meant to follow, this excludes some approaches taken by some exoskeleton devices that have implicit limitations.

These approaches to imitate the biological model are extended to the number of fingers covered by the device and on a different level to the force exerted and the reaction and movement speed, although these last two characteristics have technological limitations unlike the other mentioned that were design problems.

The joint mechanisms described show a wide range of geometrical approaches to the remote centre of rotation problem, most of which have passive adjustments for the translations component of the motion or are unadvisable for full hand applications due to discomfort or risk of injury to the user. A rigid and completely and continuously controlled method is preferable, similar to the six-bar mechanism although the mechanism profile can be lowered for better object manipulation.

Many devices have, to some level, mix operation styles, where the exoskeleton glove is able to collect instructions from the user and applies motion to the mechanism, either directly or as a response to the obstacle detected by the virtual or remote slave device. Implementing this approach to robotic operations makes it possible to simply adjust the controller software to the intended functionality expanding the devices versatility.

Due to slow neuroscience research into the motor cortex, it is still not possible to accurately and reliably identify muscle control neural signals directly from the brain. This task is made more difficult with external, non-intrusive sensors, which are preferable, to read the movement instructions directly from the source. This sensory method would be ideal to move the exoskeleton glove for use in remote operation and for patients who suffer from physical disability and are therefore unable to actuate the motion based sensors in the exoskeleton glove.

3

Supporting Concepts

The biomechanical structure of the human forearm and hand serve as the bases for the exoskeleton hand and many approaches to the development of the artificial system mimics the biological. Since nature already applied real live genetic algorithms in the development of the human arm, and associated organic systems, it is important to know the details of the resulting structure before creating an external support mechanism for it.

Skeletal Structure

Bones Tissue

Human bones present an endoskeleton architecture and perform different functions like mechanical, by protecting organs and providing support while allowing for articulated movement, synthetic, they are essential for the production of blood cells and hormones, and metabolic, mineral and fat storage and their associated release and metabolism control.

The relevant function to study in this case is the mechanical where its differentiated layered structure provides rigid support with flexible, shock absorbing, extremities and lightweight porous network interior[14].

On the surface of the bone, there is a layer of periosteum composed of two sub layers [15], the outer fibrous sub layer contains fibroblast [16], responsible for synthesising extracellular matrix and collagen that are critical in tissue repair, while the inner cambium sub layer contains mesenchymal stem cells [17] from which arise osteoblasts which in turn develop in to osteocytes, the base

material of the cortical bone and is then responsible for increasing bone thickness and repairing bone fracture, and it also differentiate in to chondrocytes [18] that are cartilage cells. This layer also has nociceptive nerve endings that make it sensitive to manipulation, provide the body with new blood supplied by the marrow and provide an attachment for muscles and tendons.

The hard outer layer of the bone, which displays its typical white smooth appearance, is composed of cortical bone [19] and it accounts for 80% of an adult human skeleton. This apparently uniform surface consists of multiple microscopic columns, called osteon [20], each of them being agglomerations of layers of osteoblasts and osteocytes formed around a central Haversian canal and remain metabolically active, as bone is constantly being reabsorbed and created, changing the location and nature of cells in the osteon. The osteon are connected to each other by Volkmann's canals at right angles to them.

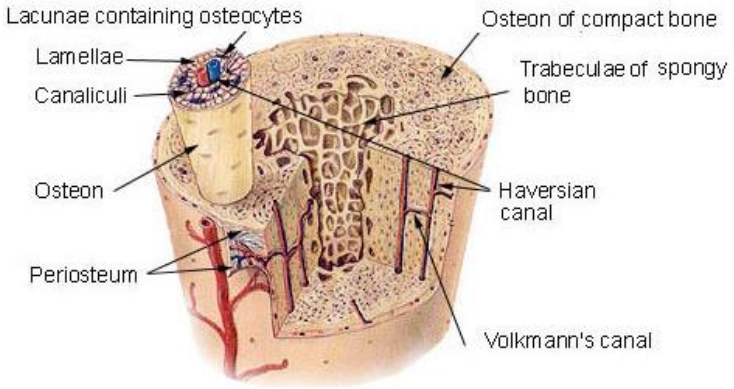

Fig 3.1: Cross-section of a human bone identifying each of its components (Taken from [21])

Inside of the cortical bone lies the cancellous bone [22], separated from the outer layers by a lamina of endosteum [23]. This layer of bone consists of thin formations of osteoblasts covered in endosteum that create the porous network of the spongy bone by forming irregular interconnection of spaces. The network structure is predominant in long bone extremities or proximal to joints, where they serve as a shock absorber of the bone due to alignment of their trabeculae towards mechanical load distribution [24], and inside vertebrae where they add to the bones structural strength.

The bone structure is similar to composite materials, particularly fibre-reinforced plastic, where fibres provide tensile strength and pliant stability, like osteon columns in bones, and are infused with plastic resins that work akin to layers of osteoblasts and osteocytes. There is still no equivalent to the perioste-

um layer that could continuously repair damaged fibres from the synthetic composed material.

In each of jointed bones endings there are layers of hyaline cartilage [25], which are a smooth rubber-like elastic tissue that forms a sleek padded surface, it also covers the cancellous bone found in long bone extremities providing the joint with a denser and near frictionless sliding surface. This material produces Proteoglycan 4 (PRG4) [26] that serves as a lubricant and abrasion protection reducing the erosion of the joint surfaces.

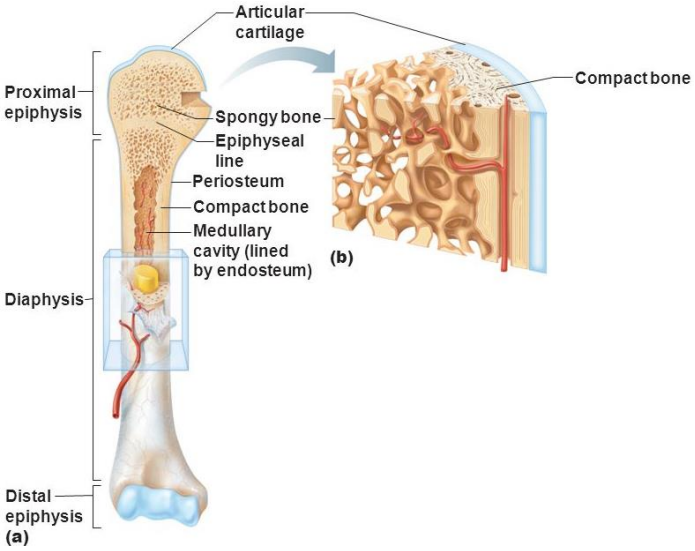

Fig 3.2: partial longitudinal slice of a human long bone with its components identified (Taken from [27])

Ulna/Radius

The ulna and radius are the two bones of the forearm [28, pp. 122–126] that connect the carpals of the wrist to the humerus and maintain hand orientation during pronation and supination, noticeably the prominence of the ulna is the defining feature of the elbow. These bones have a slight curvature that allows the radius to rotate around the ulna, this rotation of the forearm represents a rotation on the joints of the elbow of both ulna and radius bases while maintaining the alignment of the carpals the same as the changing orientation of the hand and keeping the arch where the wrist slides, while performing abduction and adduction of the hand, in the appropriate position.

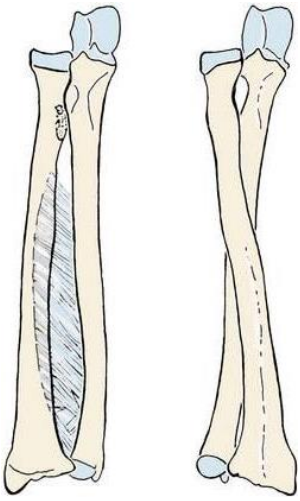

Fig 3.3: coupling of the ulna and radius bone parallel and pronated (Taken from [29])

The muscles used for finger flexing and abduction, with the exception of the thumbs thenar eminence and the little fingers hypothenar muscles, and wrist movements are located around these bones reducing the thickness and weight of the hand making it easier to manipulate objects and interact with the environment.

Carpals

There are 8 carpal bones that separate the metacarpals in the palm section of the hand from the ulna and radius in the forearm [30, pp. 126–127]. Carpals are separated in to two groups of 4, the proximal carpals juxtapose to the forearm bones and the distal carpals connected to the metacarpals. The two carpal bone groups mediate the wrist movement between the hand and the forearm bones, by having the distal carpals move to accommodate the metacarpal bones according to finger position while the proximal carpals compensate the changing combined profile of the previous carpals to surface of the arch formed in the ulna and radius wrist joint.

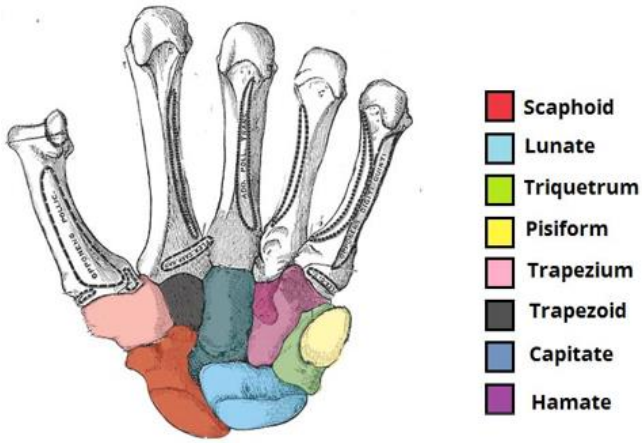

Fig 3.4: Representation of the carpal bones with their identification with the metacarpals located on top (Taken from [31])

One of the proximal carpals, the pisiform bone, is not involved in wrist movement [32, p. 5] instead providing a anchoring point for the abductor digiti minimi distancing it from the base of the little finger, thereby giving its actuation a better leveraging point, and improving the abduction motion of the finger. This is the only finger that requires such levering of the actuation muscle for the others use forearm muscles or the relative position to each other as displacement reference. This bone also forms the ulnar border of the carpal tunnel from which the median nerve emerges.

The wrist bones display a complex architecture with 7 bones dedicated to wrist movement, required due to the coupling of five metacarpals in to a single joint point composed of two separate bones, each of them with their independent movements, and the additional movement of the hand in relation to the forearm bones.

Metacarpals

In the intermediate part of the skeletal hand, between the carpals of the wrist and the phalanges of the fingers, are the metacarpals [33, p. 11]. These bones form an arch in their proximal end where the row of distal carpal bones are fixed.

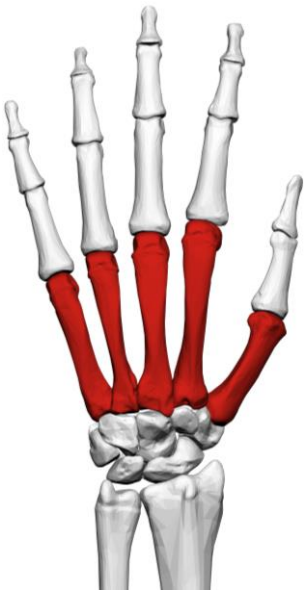

Fig 3.5: Illustration of the bones of the hand with the metacarpals in red (Taken from [34])

Between the metacarpals there are intrinsic muscle that control the abduction and adduction of the fingers [28, pp. 96–104], with the volar interossei responsible for adduction of the fingers towards the middle finger and the dorsal interossei that abduct the fingers away from the middle finger as well as ad-

ducting and abducting the middle finger. The little finger, due to being at one extremity of the hand, has a different muscle called the abductor digiti minimi, which was mentioned before in reference to the function of the pisiform. The last intrinsic muscle group located beside the metacarpals are the lumbrical, used to extend the interphalangeal joint and flex the metacarpophalangeal joints.

Phalanges

Each finger of the hand has three phalange bones, with the exception of the thumb that only has two [35, Pt. II. Osteology, Ch. 6b, Sec. 3]. These bones are considered long bones in terms of their design indicating that their structure is similar to that of the femur with an identical cancellous bone extremity able absorb vibrations, preventing possible damage to the bone, and able to perform repetitive movements with minimal detrition derived from the articular cartilage covering the sliding surfaces of the bone ends. The joints that separate each fingers phalanges and the metacarpal are actuated through the use of tendons connecting to extrinsic muscles, most of which are located on the forearm.

Fig 3.6: Illustration of the bones of the hand with the phalanges in red (Taken from [36])

The phalanges have several sheaths [28, pp. 96–104] to hold tendons close to the bone in the palmar side during flexing and to detain them from sliding tangentially to the finger on the dorsal side of the hand. The space left between the bone and the flexing tendon serve as an additional levering distance to actuate additional joints in the tendons path. This system of sheaths to extend the actuation to other joints is also used in the wrist where the flexion or extension movements of the finger will also influence the movement of the wrist when the fingers encounter resistance or obstacles to their movement.

The wide and flat expansions in human distal phalange are called apical tufts [37] and it is different in their shape in comparison to other animals due to their having cone shaped distal phalange extremities. This differentiation of the fingertip of humans makes the skeletal hand particularly adapted for pad-to-pad precision grasping improving their use in detailed and delicate operation of tools and objects.

Muscle Operation

Human muscle works in the principle of microfilament contraction [38]. The activation of the excitation-contraction coupling relies on key proteins that form a triad [39, p. 124]. The sarcoplasmic reticulum (SR) [40, p. 69], a structure that stores calcium ions, is surrounded by ryanodine receptor that releases the ions stored in the SR when stimulated by ions from synapses signals originated in motor neurons or from other SR. This calcium storage proteins are located on either side of dihydropyridine receptors, a component of the surface sarcolemma and transverse tubule, which serve to spread electrochemical signals, in the form of calcium ions, thru the outer surface of bundles of myofibril permeating other SR causing a flood of calcium ions in the muscle.

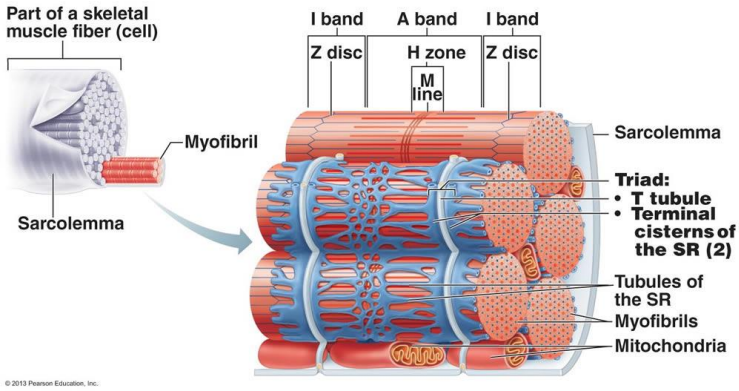

Fig 3.7: Section of the skeletal muscle with each sub-level components (Taken from [41])

When the calcium released in the action potential [42, Pt. II: Cell and Molecular Biology of the Neuron], which is small and quick impulse of electrochemical signal in this case made of calcium ion, permeates the myofibril membrane [38] and is spread inside the muscle fibres it triggers a near synchronous activation of thousands of calcium sparks. The rapid increase of calcium in the myofilaments [43, pp. 1–120] gives rise to the upstroke of the calcium transient that lead to the contraction of the myofibrils. The increase in intracellular calcium concentration causes the calcium in the cytosol, the main component of the intercellular fluid, to bind to the Troponin C by the actin filaments.

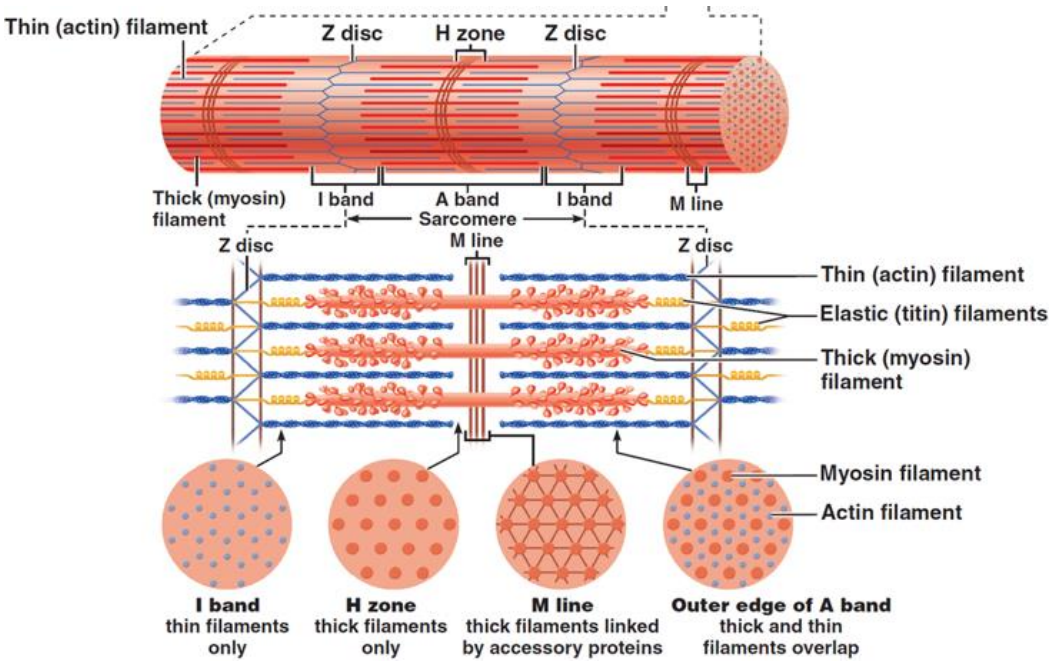

Fig 3.8: Ilustration representing the internal structure of the myofibril (Taken from [44])

Myofibril are composed of long proteins including actin [45], myosin [46], and titin [47]. Myosin are adenosine triphosphate-dependent (ATP) [48][39] motor proteins responsible for actin-based motility that are shaped in a two tailed coiled-coil morphology with two heads. According to the sliding filament theory the myosin proteins walk along the adjacent actin-based thin filaments when subjected to the proper chemical signals.

Sliding Filament Theory

While at rest the myosin is bonded to an ATP molecule and its heads are separated from the actin filament due to the presence of tropomyosins filaments between them [49], [50]. When calcium ions are introduced in to the system they bind to troponim C causing the tropomyosin filaments to slide over the actin binding site unlocking them which result in both myolin heads to close and binding strongly to them creating a crossbridge.

The attachment of the myolin to the actin causes ATP hydrolysis [48] that releases the inorganic phosphate and initiates the power stroke. After the shortening of the sarcomere the myolin head releases the remaining adenosine diphosphate (ADP) there is a further slide of the actin filament inward but the myolin head remains firmly attach. The contraction of the myofibril remains until there is a new insertion of ATP molecules, the absence of this renewal is

what causes rigor mortis, but once that occurs the myolin heads detach from the actin filaments as the calcium ion levels in the cells are regulated and the tropomyosin return to place blocking the acting binding sites ending the cross-bridge cycling [51, Ch. Chapter 34: The Motor Unit And Muscle Action].

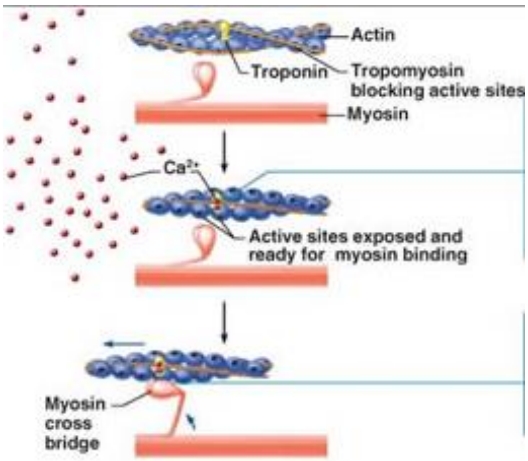

Fig 3.9: Diagram of the sliding filament theory actuation (Taken from [41])

Similarly to the biological muscles the pneumatic artificial alternatives have a constant supply of energy, in the latter case not of ATP but of compressed air, and are contracted when exposed to an energetic signal, in the biological version it's a calcium ion that serves the same purpose as that of the electrical signal of the artificial mechanism. The main difference in the functional comparison of both systems is that the organic muscle has energy stored inside of it while at rest and the artificial muscle receives its energy after the valves receive the actuation signal.

Muscle Mechanical Attachment

Muscles are both connected to and continuous with the tendons that are, in turn, connected to the periosteum layer surrounding the bones [52]. The tendons are made of type 1 collagen, the same as bone, skin and organs, and connect to the muscle at the myotendinous junction whose extracellular matrix main components include laminin, integrin, vinculin, fibronectin and talin, which enable a strong connection between the muscle actin filaments and the tendon collagen fibres [53]. There are also Golgi tendon organ present in the junction between muscle and tendon which are a sensory receptor that senses muscle tension to better control muscle actuation.

The biological tendons are able to "slide" beneath the surface of the skin maintaining their connection to neighbouring tissues avoiding friction and interference with other systems [54]. An artificial mechanism however requires a

protective sheath containing an internal surface that reduces attrition and an external non-compressible structure to allow for the mechanical force to be transferred from the actuator to the intended destination.

Nervous System

Sensory System

In biology, environment perception is provided by sensory receptors composed of different sensory neurons that react to stimulus and react with electrochemical signals [55]. Like all neurons they collect stimulus through dendrites [56, pp. 20–36], the input ports of neurons, but in the case of sensory nerves these branched projections transduce external stimuli in to action potential by increasing the permeability to sodium ions, similar in function to calcium ions used in muscle contraction but are at least 100 times faster, in the cells membrane, meaning sodium channels will open up causing the propagation of an electrochemical impulse thru the axon, the output port of the neurons, of the nerve cell in to the next synapse and so on in to the brain cortex. Mechanoreceptor, touch mechanical sensors, are able to react to physical stimulus with the opening of the sodium ion channels in exposed dendrite membrane.

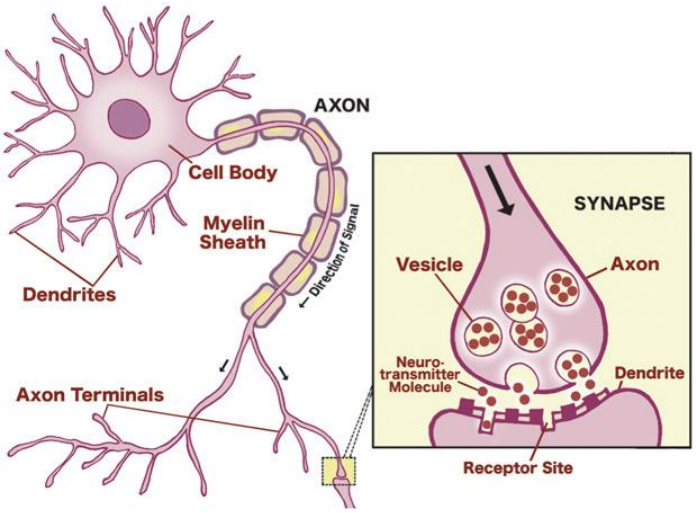

Fig 3.10: Illustration of the structure of a neuron and its synapse (Taken from [57])

Mechanical tactile sensation in humans is divided in to four major sensory receptors: Pacinian corpuscles, sensible to vibrations, Meissner's corpuscles, which detect light touch, Merkel's discs, responsible for detecting pressure and deep static touch features, and Ruffini endings, which sense skin stretch.

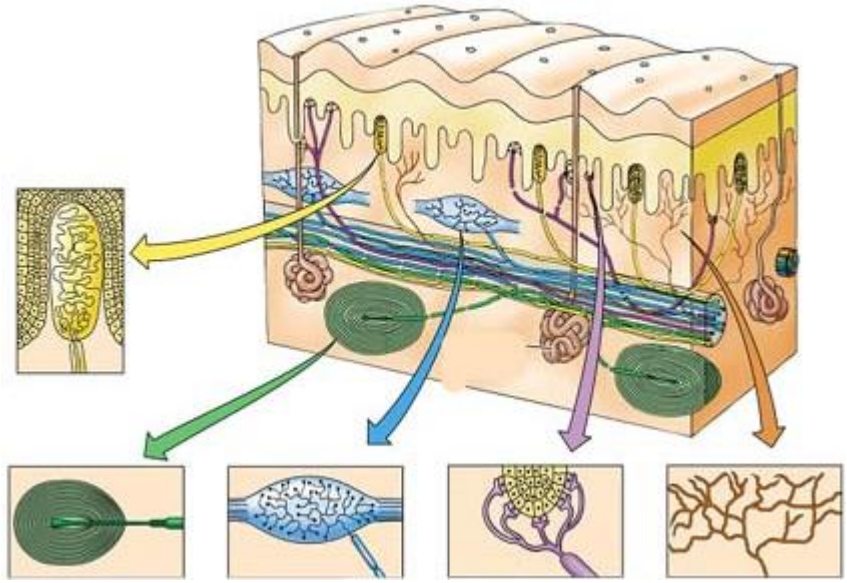

Fig 3.11: Illustration of the sensors located on the human skin with the Meissner's corpuscle on the top left, followed by the Pacinian corpuscle under it, the Ruffini corpuscle on its right, the Merkel's disc on its right and lastly free nerve endings (Taken from [58])

Pecinian corpuscles respond only to sudden disturbances making it especially sensitive to vibrations [59], this makes it possible to identify textures thru the vibrations resulting from sliding the finger on a surface. Groups of corpuscles are able to detect deep pressure changes, like for instances when interacting with objects. This sensor is formed in the shape of concentric capsules with 20 to 60 lamellae, made of fibroblasts and fibrous connective tissue, with gelatinous material inside of them consisting of more than 92% of water. Inside the concentric capsules there is a neurite of a single afferent unmyelinated in the sensing area, making this section uninsulated due to the absence of the myelin sheath.

Meissner's corpuscles [60, pp. 7236–7246] are rapidly adaptive receptors with low threshold, ideal for detecting light touch displaying their highest sensitivity when stimulated with vibrations between 10 and 50 Hz. These corpuscles are formed as capsules of connective tissue with unmyelinated nerve endings in spiral coils inside of it and supportive cells arranges in horizontal lamellae.

Merkel's discs, unlike the previous two sensory receptors, have slowly adaptive unencapsulated receptors having instead their nerve endings myelinated, which results in their sustained response [51]. Each afferent nerve fibre branches to innervate up to 90 endings. With their slow rate of adaptation they

sense physical disturbances at low frequencies, around 5 to 15Hz. The proximity of these touch sensors to the surface of the skin makes them sensitive to smaller tissue displacement, of less than 1µm, and with the same nerve fibre innervating up to 90 endings gives it a smaller receptive field than the other sensors, those characteristics result in a higher resolution tactile discrimination, used for detecting fine surface patterns, like when reading Braille.

Ruffini endings [61, pp. 149–156] are slowly adaptive enlarged dendritic endings with a cigar shaped capsule sensitive to skin stretch. They are able to respond to sustained pressure with very little adaptation. Being primarily used to help with object interaction, for example helping control slippage of grasped objects, they are located in greater density around finger nails, where they have a fixed reference point to sense the amplitude of skin stretching.

These sensors distribution form a network capable of detecting a wide range of mechanical stimulus with different precision, frequency and depth of pressure. The combination of sensory information help to complement each sensory receptors limitations improving the detection, identification and interaction with the environment and distinct objects.

Sensory Information Transfer

After the sensory data collection, by the sensory receptors that form the first order neurons, the electrochemical signals are transmitted thru synapses to the dorsal column nuclei, the second-order neurons or sensory track where it decussates, meaning it changes to the opposite side from its entrance location, to the thalamus [62], a major relay station for sensory information, where it synapses to the third neuron in the sequence [63], in the ventrobasal complex, before being projected to the somatosensory cortex.

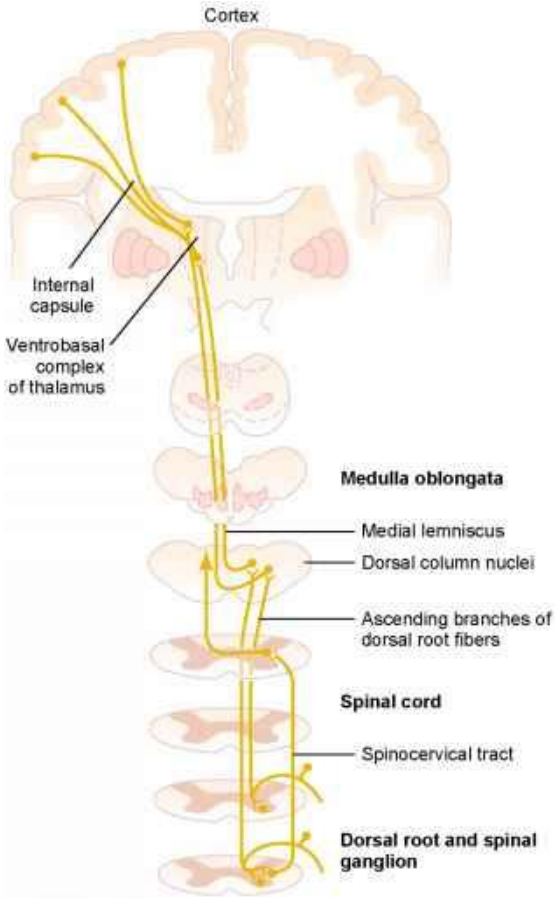

Fig 3.12: Illustration of the path of the nervous signals to the brain (Taken from [64])

The section of the brain dedicated to touch processing is the primary somatosensory cortex located in the lateral postcentral gyrus which is a narrow band that runs from each side of the brain thru the top centre of the head and is the frontal section of the parietal lobe [65]. This cortex is bounded rostrally by the primary motor cortex and each side of the hemisphere corresponds to the opposite side of the body. In this space there is a map of the sensory areas called the sensory homunculus that associates each body part to a specific group of neurons in the cortex, the list of body parts starts in the centre of the brain with the genitals then follows from toes to head and then to the hand and fingers ending in the face and constituent parts[66]. The area of the brain dedicated to each body part is proportional to the sensitivity of that body part instead of their actual relative body size.

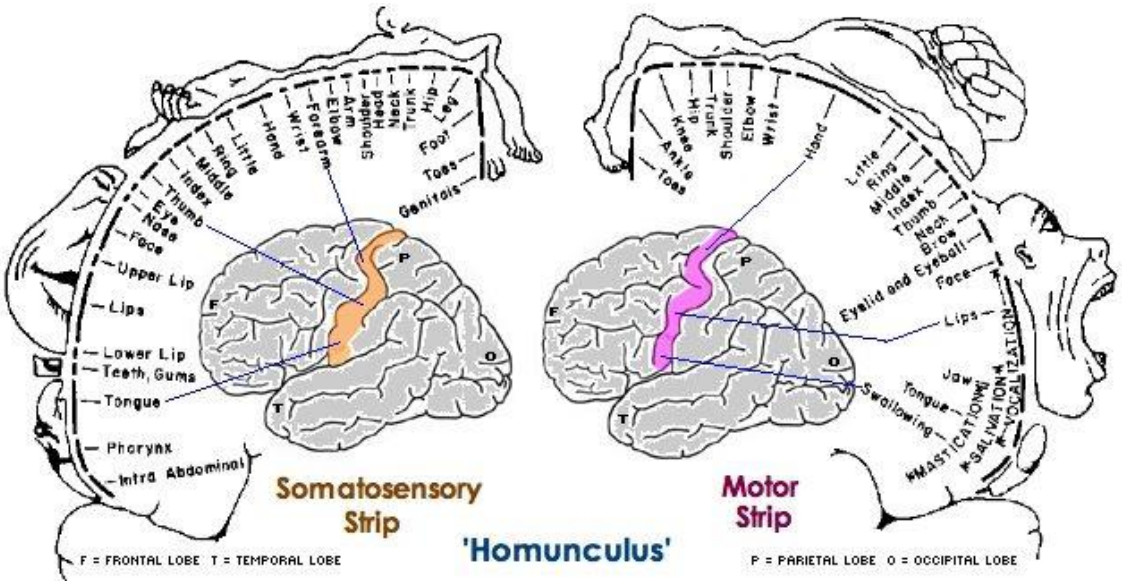

Fig 3.13: Illustration of the somatosensory and motor strips and their respective cortical homunculus (Taken from [67])

In the primary motor cortex there is an identical cortical homunculus to that of the primary somatosensory cortex with similarly placed association of body parts [68], meaning that the part of the brain that controls the hand is located next to the part of the sensory cortex that processes touch sensation from the hand. The proportions of each body part of the cortical homunculus in the motor cortex differ from the proportions of the somatosensory cortex.

Neural Signal Processing

When the signals from the sensory receptors reach the brain they are projected on to the neurons of the nearest layer of the section of the somatosensory cortex associated with each specific sensing region [69]. These neurons are arranged in the sensory cortex in layers where the signals from the thalamus are projected in to layer IV which in turn project into other cortical layers, the neurons are grouped together with similar inputs and responses into vertical columns across layers that progressively process the sensory information.

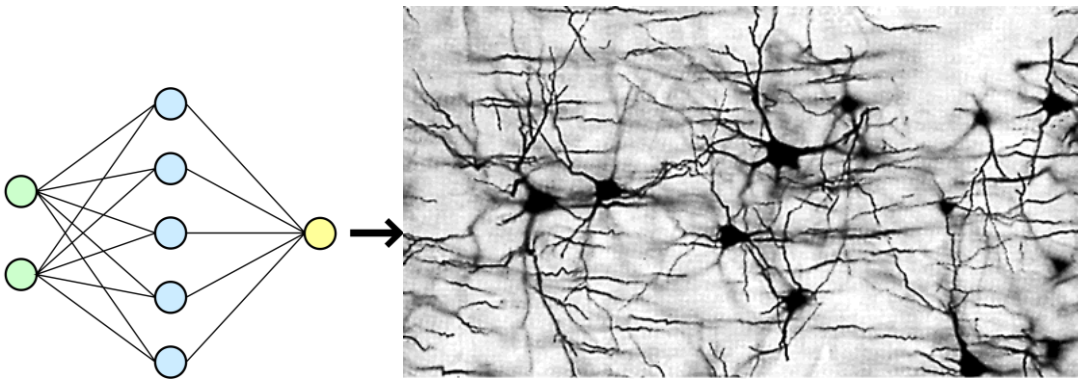

Fig 3.14: Logic diagram of a neural network on the left and a picture of a natural neural network (Taken from [70], [71])

When a specific neuron collects sensory information in their dendrites it adds the sensory input until it reaches the threshold potential that causes the voltage-gated ion channels to open causing a propagation of the signal in to axons that synapse them to other neurons [72]. The operation procedure inside each neuron works on the bases of collecting impulses from enough axioms to cross the threshold potential causing the depolarization of the membrane potential releasing a new action potential to further connectors.

To exemplify a neuron responsible for detecting a specific object, like a grain of sand, will collect the signals from neighbouring neurons responsible for detecting each characteristic, its hardness, the size, the texture, the weight and so on, and if all of them are activated then this neuron will trigger an action potential meaning that it was positively identified has that specific object. Studies have revealed that different action potential frequencies cause neurons to propagate the signal into neurons in different directions depending on their preferred direction [73].

Comparing the thought process of sensory input of the brain shows that a progressive decoding of the information takes place through consecutive layers of simple processing units instead of a singular powerful and complex entity. This can be compared to the way processors work, they are a conglomerate of transistors that redirect input signals thru a designed network to arrive at a particular output instruction, but they are seen conceptually as an compact entity, just like the brain.

Muscular Anatomy

Starting in the hands there are some muscles used to actuate the different movements performed by the metacarpals of the fingers, except the thumb whose metacarpal extension and abduction are located on the forearm [74].

The muscles that exclusively move the metacarpal of the little finger are collectively called hypothenar muscles and consist of abductor digiti minimi, that as indicated by the name abducts the little finger, flexor digiti minimi brevis, dedicated to flexing of the little finger, and opponens digiti minimi which rotates the little finger towards the centre of the hand making it possible to touch the thumb [75].

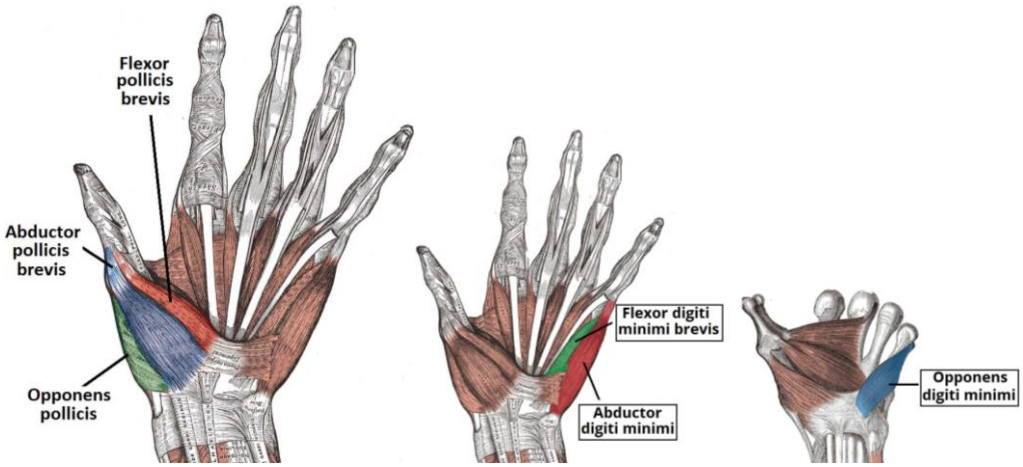

Fig 3.15: Illustration of the thenar and hipotenar muscles of the hand (Taken from [76])

To rotate and flex the metacarpal of the thumb the hand has a group of muscles called thenar eminence containing three muscles named abductor pollicis brevis, responsible for abducting the thumb, flexor pollicis brevis, actuates the flexion of the metacarpal of the thumb, and the opponens pollicis that rotates the thumb towards the centre of the hand placing its distal phalange in the path of the remaining fingers [77].

Abduction and adduction of the fingers is left for dorsal interossei, that abducts the fingers away from the middle finger as well as abducting and adducting the middle finger [78], and the palmar interossei, responsible for adduction of the fingers towards the middle finger [79].

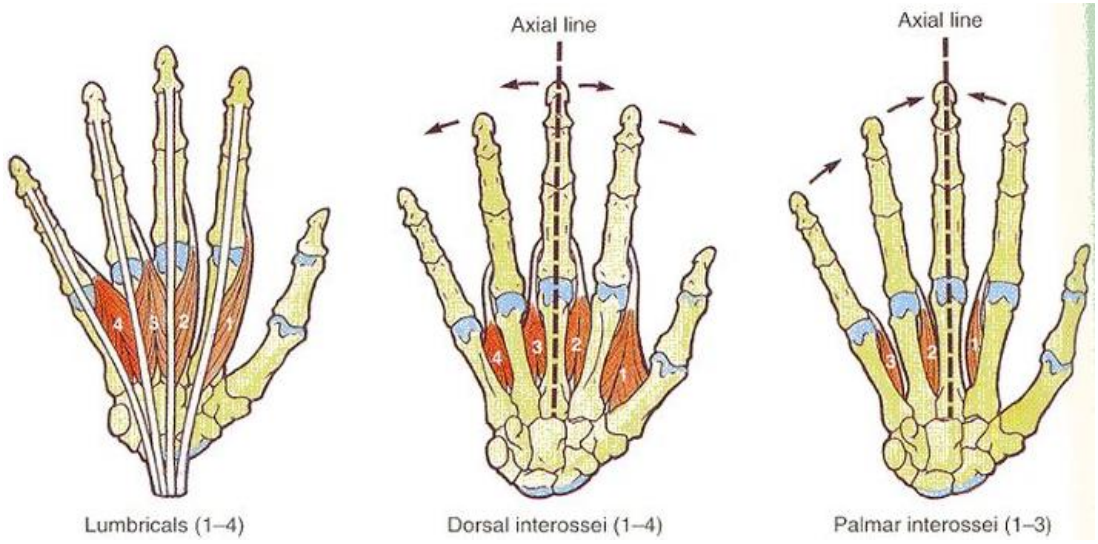

Fig 3.16: Illustration of the dorsal and palmar interossei and the lumbrical muscles (Taken from [80])

The flexing of the metacarpophalangeal joints independently of the proximal interphalangeal joints can be accomplished thru the use of lumbrical muscles that instead of acting directly on the bones, like most skeletal muscles, are connected to other tendons and ligaments making it possible to flex the metacarpophalangeal joints while extending the proximal interphalangeal joints [81].

In the forearm there are 19 muscles responsible for movements of the hand and fingers, 6 are dedicated for wrist movements, 4 move the thumb, one exclusively for the index finger and another for the little finger, tree to move all four fingers, thumb excluded, and 4 are used to move the forearm.

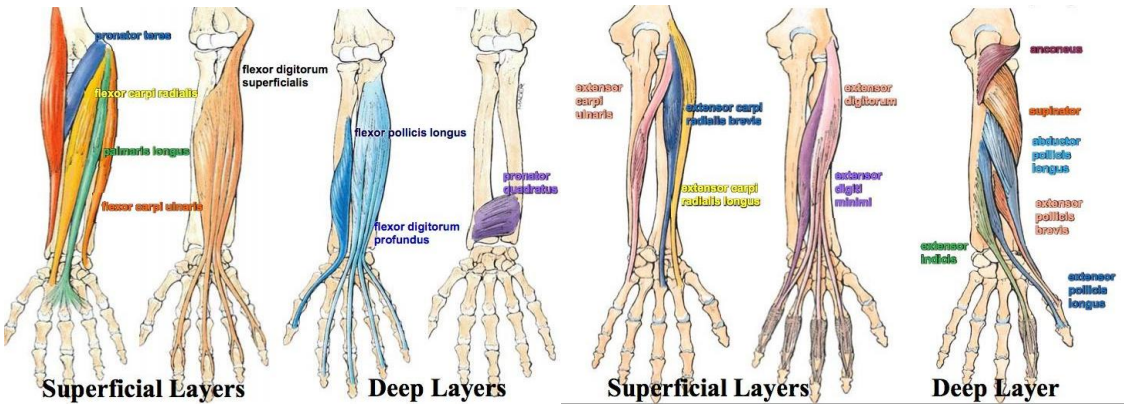

Fig 3.17: Illustration of the muscles of the forearm separated by depth layer with the anterior section on the left and the posterior compartment on the right (Taken from [82])

To move the fingers in an extending direction there is a group of muscles partially blended together identified singularly as extensor digitorum [83]. Due to the pulling effect being made from the forearm to the fingers the actuation of

this muscle can also apply force to extend the hand when the fingers do not, or cannot, extend any further. The blended aspect of this muscle and the finger flexing muscles compromises the actuation independency of the fingers limiting the singular digit extension or flexion to a reduced amplitude before it begins to affect the neighbouring fingers.

For finger flexion there are two muscle groups responsible for different joint actuation. This separation of movement actuation is necessary to make it possible to provide a larger number of degrees of freedom to the phalanges and is accomplished by limiting one muscle group, the flexor digitorum profundus located in the deep layer of forearm muscle, to the distal interphalangeal joints and another muscle group, the flexor digitorum superficialis located in the superficial muscle layer, to the proximal interphalangeal joints [84].

The nerve that act the section of the 4th and 5th fingers on the flexor digitorum profundus is the ulnar nerve while the section of the muscle that flexes the other two fingers is the median nerve, the same that acts the flexor digitorum superficialis, this helps to separate the movement of the fingers reducing the cross actuation of the little and ring finger to the middle and index fingers [85].

The thumb has a different muscle architecture in comparison to the other fingers in that it has separate muscles responsible for flexing, the flexor pollicis longus, another for abduction, the abductor pollicis longus, and two muscles dedicated to extend the thumb exclusively in the metacarpophalangeal and in combination with the interphalangeal joints, respectively the extensor pollicis brevis and the extensor pollicis longus [86, Ch. Chapter 9: The Wrist and Hand Complex].

By analysing the actuator distribution of the human hand it is noticeable that there are coupling of joints to the individual muscles that, even so, are able to move independently with the help of combination of antagonistic actuations from other muscles. This reduces the number of required muscles while keeping the freedom of movement by increasing the systems complexity.

The muscles that have the biggest influence in the topographical change the surface of the forearm are the external muscles in the posterior compartment of the forearm [87]. This muscles are the brachioradialis, responsible for elbow flexing along with pronation or supination depending on the position the

arm is in, the extensor carpi radialis longus and the extensor carpi radialis brevis, responsible for extension and abduction of the hand at the wrist, the extensor carpi ulnaris, extends and adducts the wrist, and the anconeus muscle, that assists in the extension of the forearm also stabilizes the elbow and abducts the ulna during pronation.

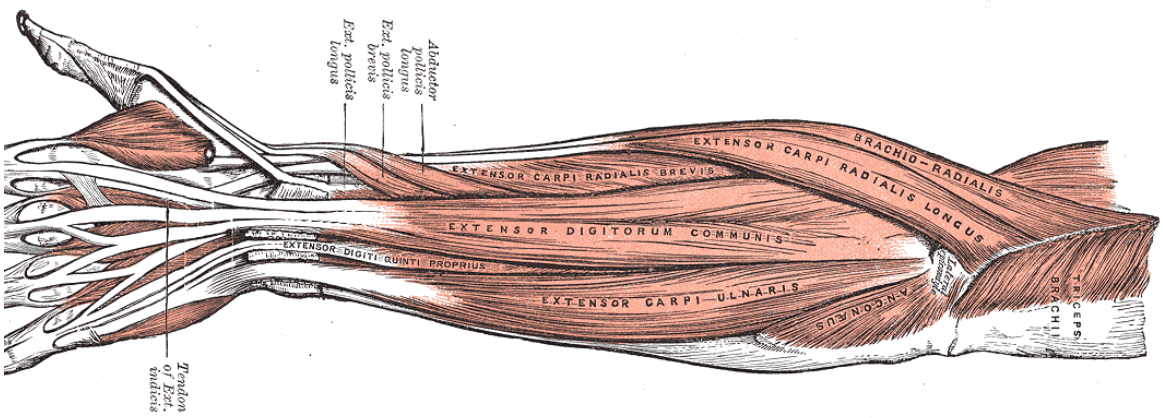

Fig 3.18: Illustration of the superficial muscles of the posterior compartment of the forearm (Taken from [87])

Contraction of the previously mentioned posterior compartment muscles changes the topography of the forearm as well has change their relative position to the wrist and elbow during wrist pronation and supination.

For the design of the exoskeleton bracer, that holds the actuation mechanism, the position of the forearm muscles influenced the location of the structural supports by displacing rigid structure away from the mobile wad muscles [88], the ones responsible for elbow flexing and the extension and abduction of the hand at the wrist, due to their volume and location on both the radial and ulnar sides of the forearm.

4

Mechanical Architecture

The idea for the development of an exoskeleton hand began with a thought exercise on how to perform the rotation and translation required for an exoskeleton finger joint with over actuation, this makes the design of the mechanical structure of the device the logical place to approach the subject.

Finger Joint Mechanism

The mechanism design for the finger joint is based on the scissor mechanism which, when all parts have identical dimensions, extends in one direction as a response to the contraction in a perpendicular direction.

To change the movement path of the mechanism the dimensions of the intersecting sections was altered resulting in a curved motion. By analysing the change in movement path associated with different dimensions a pattern was extrapolated making it possible to tune the design thru algebraic equations in to an initial working geometry.

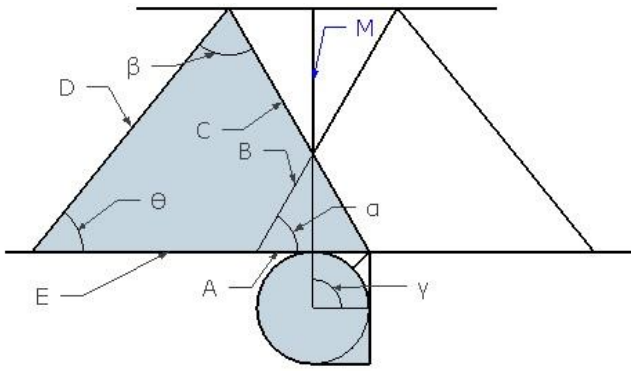

Fig 4.1: Diagram of the initial mechanical joints diagram

The initial design displayed a pronounced mechanism in the superior section of the geometry and required extensive attaching surface on both sides of the articulation. To improve this design weakness and make the protuberance less pronounced, increasing the appeal of the product for an eventual application onto a commercial product, alterations were made to the geometry intended on reducing the height of the mechanism which resulted in a curved superior leaver, composed of sections C and B.

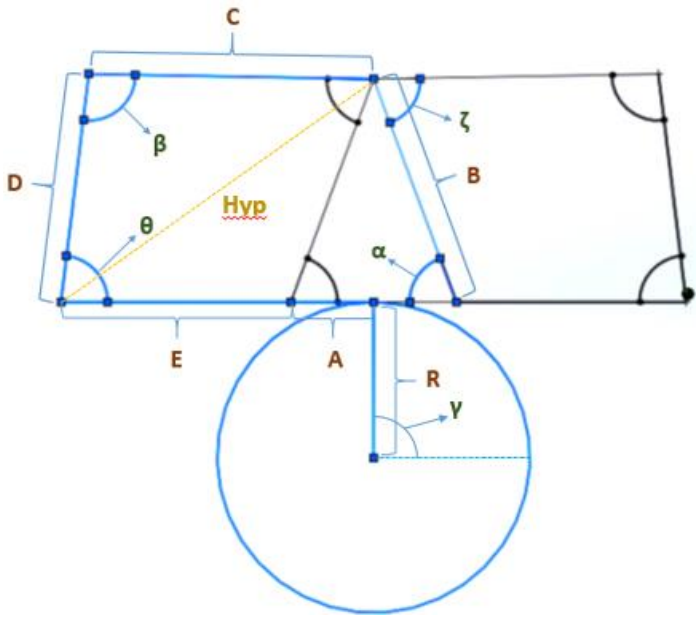

Fig 4.2: Diagram of the perfected mechanical joint geometry

The joint mechanism diagram in the above figure has indicated the relevant vectors of the improved geometry able to perform the rotation and translation required for an exoskeleton over actuated finger joint. Each of the letters represents one measurement with their own meaning:

- "R" indicates the radius of the semicircle described by the path of the join movement in relation to the remote centre of rotation;
- "A" is the distance between the edge of the finger section to the furthest rotational connection;
- "B" and "C" are de two sections of a single rigid link that connects both finger pieces over the joining edges;
- "D" the lever mechanism that imposes the desired translation and synchronises the rotation of the joint;
- "E" is the distance between the lever connections to the base and determines the correct rotational path of the movement.

The equations relating each of the dimensions and the connecting angles are as follow:

When the joint is in the flexed position the "B" link will be vertical in relation to the stationary finger section and in this position the connection ζ is collinear with that section making the dimension of B the sum of "A" and "R", as expressed by equation (4.1).

$$B = A + R \tag{4.1}$$

The angle α is set to be zero when the joint is closed, $\alpha_{final} = 0°$ required for the "B" link to be position vertically in that circumstance, and by calculating the distance to a virtual intersection of a straight line from extending "A" to the intersection of the tangent of half the angle γ, which represent the plane of symmetry of the system, it is possible to acquire the angle α from the inverse cosine of that length, depicted in equation (4.2).

$$\alpha(\gamma) = cos^{-1}\left(\frac{A+tg\left(\frac{\gamma}{2}\right)\times R}{A+R}\right) \tag{4.2}$$

To attain "D" it is required to define the length of E, by applying the Pythagorean theorem and considering D the hypotenuse of this equation, the height of the connecting point of C with D, specified by equation (4.3), as one of the remaining sides and the difference between the horizontal position of this connection and E, depicted in equation (4.4), as the last side left we get equation (4.5).

$$B \times \sin(\alpha) + C \times \sin(\alpha - \zeta) \tag{4.3}$$

$$C \times \cos(\alpha - \zeta) - A - E \tag{4.4}$$

$$D = \sqrt{(C \times \cos(\alpha - \zeta) - A - E)^2 + (B \times \sin(\alpha) + C \times \sin(\alpha - \zeta))^2} \tag{4.5}$$

The ideal dimensions for the "A", "E", "C" and the angle of "ζ" are the result of particle swarm algorithm calculations, in appendix A, based on the equations relating all of the pieces of the mechanism and limitations imposed by the available space and specific user finger proportions. In addition to the deduced associative equations several angle and distance calculations are included in the algorithm necessary for error calculation.

By using swarm partible algorithm to calculate these dimensions it is possible to evaluate the error of the remote centre of rotation of the external finger joint for 600 combinations of the four variables of the equations described above in each iteration. The initial values of each variable is randomly selected within a set upper and lower boundaries. These boundaries relate to the size of each finger section of the users hand. Between iterations, each particle will adjust the values of its variables towards a combination of the best result observed by itself and the best result observed by the swarm. After a maximum of 600 iterations, fewer if the particle movement inside the four dimensional space has stagnated, the values for the variables that has been determined by the swarm to be closest to ideal are presented to the user.

After multiple interpolations, the algorithm returned a combination of dimensions, shown in table 4.1, that, when used to create the specific joint mechanism, reduces the remote centre of motion error to imperceptible margins, under 0.1 mm maximum error. For each joint, there are new parameters of finger length and thickness that require a new application of the algorithm for each joint installed in the system.

Table 4.1: Dimensions of each section of the finger joint mechanism

		metacarpophalangeal joint	proximal inter-phalangeal joints	distal interpha-langeal joints	Units
Index Finger	A	2	2	2	mm
	B	22	16.5	16	mm
	C	21.3312	5.9037	8.048	mm
	D	20.31735845	15.84802889	84.68237807	mm
	E	19.641	5.249	89.34	mm
	R	20	14.5	14	mm
	ζ	89.07201883	88.77408078	88.70532584	º
	Max Error	0.096	0.093	0.099	mm
Middle Finger	A	2	2	2	mm
	B	22	16.5	16	mm
	C	35.596	11.4906	10.984	mm
	D	19.30024088	15.26292087	14.77890114	mm
	E	32.872	10.246	9.754	mm
	R	20	14.5	14	mm
	ζ	89.0032639	88.716785	88.6652188	º
	Max Error	0.094	0.09	0.089	mm
Ring Finger	A	2	2	2	mm
	B	22	16.5	16	mm
	C	23.0604	13.75605	12.3632	mm
	D	20.18149477	15.03564019	14.63516355	mm
	E	21.232	12.281	10.988	mm
	R	20	14.5	14	mm
	ζ	89.08347799	88.68813711	88.64803006	º
	Max Error	0.098	0.091	0.092	mm
Little Finger	A	2	2	2	mm
	B	22	16.5	16	mm
	C	19.5052	8.052	6.6704	mm
	D	20.45274044	15.61866245	15.24171361	mm
	E	17.95	7.166	5.908	mm
	R	20	14.5	14	mm
	ζ	89.08347799	88.75689204	88.72251458	º
	Max Error	0.097	0.091	0.098	mm

Other Moving Joints

Abduction and adduction movements of the proximal carpals of the fingers are provided by revolute joints located under the preciously described over actuated joint mechanism placed perpendicularly to the centre of rotation of the metacarpophalangeal joints, on the surface of the opisthenar area, which is the surface opposite to the palm.

The thumb has one over actuated joint where the metacarpophalangeal articulation is actuated, that provides its flexion and extension movements. The other joints of the thumb have revolute joints placed concentrically to the rotation centre, this is a more advantageous joint mechanism in this particular application due to the low profile and stability characteristic of this design. The drawback that made it impracticable to be used on the other fingers are avoided in this digit thanks to its distance to the neighbouring mechanism avoiding mechanical interference and maintaining the comfort and safety of the user

Bracer Structure

The frame of the bracer is the support for the actuators, valves and controlling circuits in the developed exoskeleton and for that reason the architecture of this section of the device has to be strong enough to hold the mechanisms associated with the robotic hands active movements and resist deformation when subjected to it.

To make the device easy to install the inferior quarter of the posterior section should be clear of obstacles to allow for the user to adjust the hand position in the exoskeleton glove. An increase device comfort is provided by allowing natural ventilation of the arm through reduced structure coverage reducing the critical supports area to long and narrow links connecting the posterior and anterior rings, through which the wrist and near elbow forearm are attached respectively.

Integrity of the structure when subjected to varied mechanical forces is a result of careful positioning the few remaining supports in locations that experience increased pressure and redirecting that mechanical stress to the elbow section of the device and balancing the torsion forces with symmetrical angular junctions. This structural web was placed with attention to the changing muscle topography of the forearm to avoid unnecessary intersections of contracting muscles with rigid attachments. In the figure it is visible that the space between the bracer structural links circumvents the mobile wad that protuberates the furthest during arm movement.

Fig 4.3: Illustration of the bracer device placed over the muscle diagram of the human forearm (Forearm muscle diagram taken from [89])

The top plate provides extra support for the wrist operation while the arches around it avoid the changing volume of forearm muscle contraction, as well as providing air flow to the users' skin. Opposite the top plate there is an open space intended to help with the placement and removal of the device.

Tests of a virtual prototype of the bracer were performed for stress and torsion analysis were it was subjected to a force of 980 N, equivalent to 100Kgf, applied to the wrist wring section of the bracer and to a torque of 9.80 N/m, again equivalent to 100Kgf/cm, twisting the same section of the device. The parameters selected for the simulation are beyond the expected operating conditions of the device and are intended to guarantee its reliability even when under unusual or extreme circumstances.

Results of the stress test indicated that the expected maximum pressure experienced by the bracer, under similar circumstances to that of the simulation, would be 0.96 MN/m^2, which is under the specified maximum compressive strength for carbon fibre reinforced epoxy material of 1.1 MN/m^2, presenting a deformation of under 1cm.

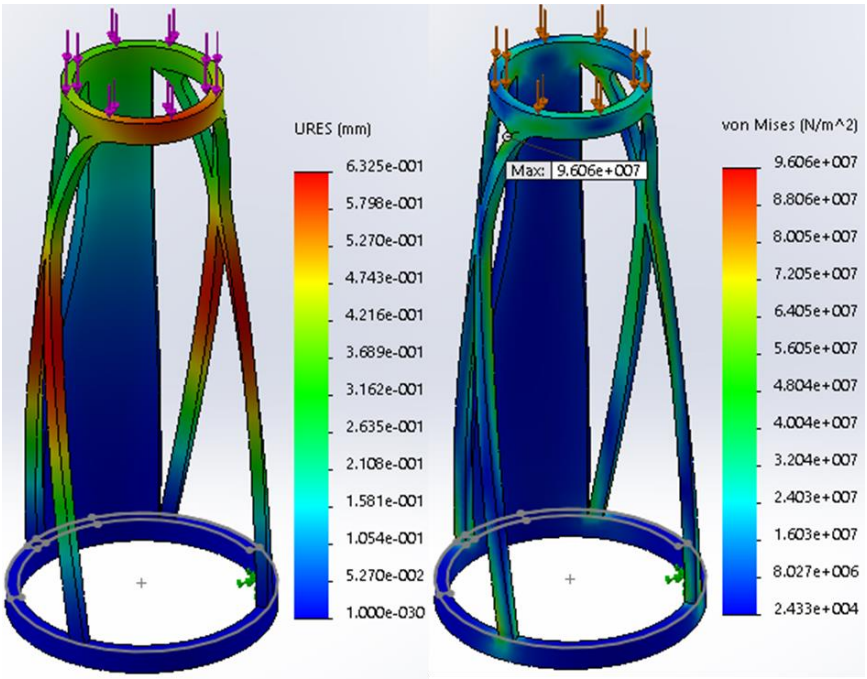

Fig 4.4: Colour graded diagram of the statical analysis of the bracer by deformation, on the left, and stress, on the right

The torsion analysis of the bracer indicated that it would experience less than half the pressure measured in the stress test having a maximum pressure of 0.41MN/m2 as well as sowing less deformation as well.

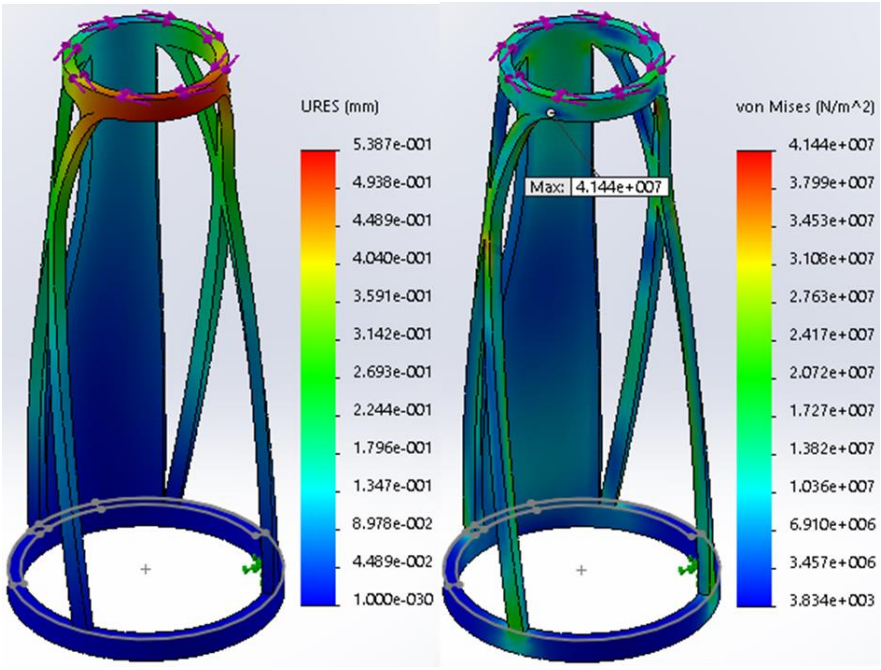

Fig 4.5: colour graded diagram of the torsion analysis of the bracer by deformation, on the left, and stress, on the right

Adjustments of the architectural design of the bracer were made to attain these results and are the result of adjustments to the structural link angles and position intended to increase durability while maintaining a reduced arm coverage and strategic openings to prevent interference with regular limb operations.

The ergonomic design of the bracer is able to support the mechanical structure of the exoskeleton glove while providing a mounting surface to the actuators and control systems. This combination of features enables the device to be a self-contained system with all the processing and actuating components located on the device structure, with the addition of an air tank and a power supply, possibly as a backpack combo, the device can be operated without any external connections.

Critical analysis

The design of the mechanical and support structures described in this chapter achieved two important objectives indicated in chapter 1. The separation of each finger articulation into independent external joints allows for differentiated actuation of each movement vector of the hand. With the bracer structure providing support for the exoskeleton glove and mounting surface for the actuating and control systems it is possible to aggregate all the components of the device, making it self-contained.

5

Actuation

Pneumatic artificial muscles were chosen to make the actuation system resemble the equivalent biological mechanism. This linear actuators are more elastic and flexible than the alternative with the added advantage of having a better power to weight ratio, being able to increase the speed and force of its movements by changing the air supply pressure and regulating the air flow.

Artificial muscles

The operation of the pneumatic artificial muscles is based on the expansion of an internal elastic tube when supplied with compressed gas, which will increase the volume of the enveloping tense braided sleeve resulting in its contraction. This reduction in muscle length in response to increased diameter under pressure is comparable to the operation of human muscles making them a good artificial replacement for the device.

Different diameter and length pneumatic muscles were made to study how these dimensions might influence the muscles performance. It was determine that the diameter influences the force of the muscle. A wider muscle has a larger radial surface subjected to pressure that is translated in to a stronger contraction.

Longer pneumatic muscles were identified as performing larger contractions due to the contraction process that reduces the sleeves length by a certain percentage. This is not a linear variation as the diameter is fixed the maximum volume will correspond to different contraction percentage depending on muscles length.

The size was selected based on the small strength needed for each finger joint, the short actuation length required to actuate each joint and the limited space available for each muscle on the bracer in order for the device to contain all its components over the users arm.

In order to provide the same number of degrees of freedom to the exo-skeleton glove that can be experienced in an average human hand in the a standard disposition requires two pneumatic for each degree of freedom. To decrease the number of actuators required without reducing the number of degrees of freedom requires a different approach to the actuation of the joints. For that end inspiration was taken from the biological model with regards to the cross actuation of multiple joints. By dividing the actuators force between two consecutive joints and keeping the opposite motion of each of those joints separate the actuation can be combined to extend or flex one of them while restricting the motion of the coupled joint by applying an opposite actuation.

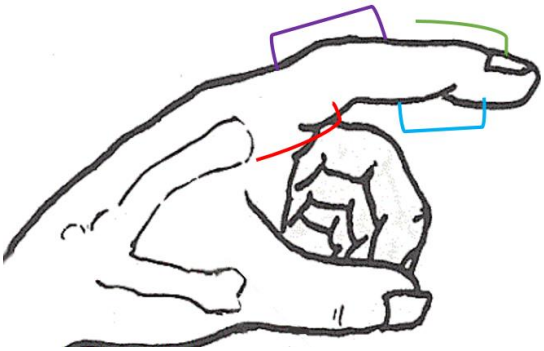

Fig 5.1: Illustration of the human index finger with indication of the actuation location (Taken from [90])

The coupling of sequential joints are organized in the method displayed where the extension of the proximal and middle phalange, in purple, is balanced by the independent actuation of a flexing actuator attach to the proximal phalange, in red, and along with the coupled middle and distal phalange flexing actuator, in blue, cross balance the force distribution to the middle phalange leaving the last phalange to be actuated for the extending motion by a dedicated muscle, in green. This disposition of coupled articulations allows for more actuators to apply force in the grasping motion of the proximal and middle phalange where this pressure is most important to interact with objects.

By alternating between contraction and extension actuator coupling, and some additional dedicated actuators to cover the neglected joints, the number of actuators is reduced by at least 28% for the finger actuators.

Each actuator is installed in their own individual support structure that is able to hold the pneumatic muscle and the connecting cable with their respective Bowden sleeve with adjustable tension to allow for individual detailed adjustments to the actuators specifications.

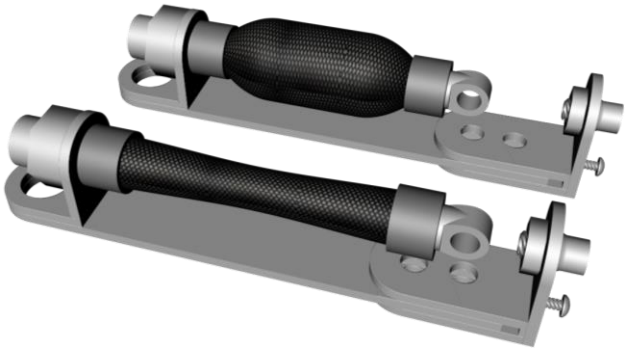

Fig 5.2: Two pneumatic muscles installed in their specific supports

The shape of the artificial muscle support base provides the required structural strength to maintain its profile even when exposed to the combined compression forces exerted by the pneumatic system and external factors. The floating extremity of the structure allows for length alterations to adjust the tension of the Bowden cable and has an attachment system to hold the force transfer mechanism to be secured.

This muscle support system makes them easier to replace and allows adjustments to be made to the system by adding and removing muscles, changing the devices performance or adding different functionalities.

It was decided that, for the prototype, bigger pneumatic muscles were better suited, due to the larger size of the joint mechanism installed in the prototype, that required longer contractions. Therefore, the prototype muscles have got 15cm length in its contracting section. The contraction length of these muscles was tested under different pressures and with a range of load weights to determine the response of these actuators under different working conditions, as shown in figure 5.3.

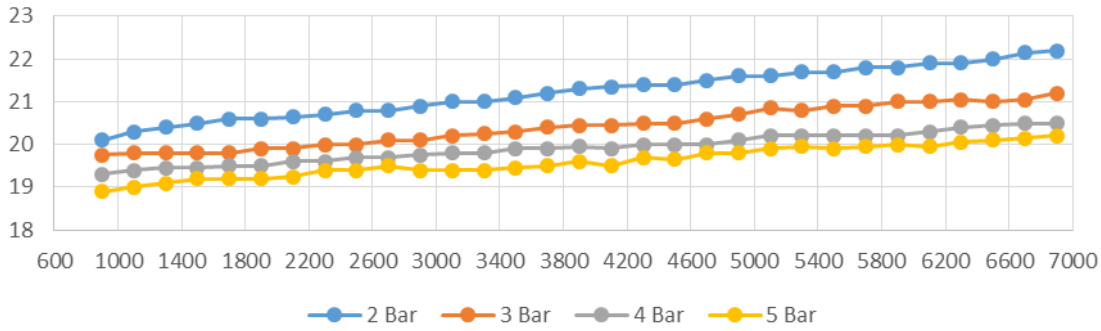

Fig 5.3: Length of the artificial muscles with different pressures when subjected to a weighted load.

The measured length of the muscle and its structure while empty was 23.4 cm. Al measurements start with a load of 900g from the vessel used to hold the weights being added during the test. As expected, the chart in figure 5.3 shows that with increased pressure the muscle extends less for each additional load than the same muscle with less air pressure. The detailed data collected from the experiment is in appendix D. These results show that the mechanism is capable of lifting, with a single actuator, more than 6kg. Considering that the muscle length only influences the contraction length, this experiment demonstrates that each single muscle is easily able to surpass the strength of an individual human forearm muscle.

Measurements of the reaction time of the artificial muscle proved to be difficult and unreliable due to the very fast contraction speed observed when inflating the muscle. This muscle contraction when applied to a finger joint, with 4 bar pressure and unrestricted air flow, exceeds the users grasping speed.

Valves

To increase the movement precision of the actuator there were three possible approaches to the air supply management:

- **Directional Control Valves**, with limited control, being only able to commutate the fluid or gas supply between the stationary and an alternate outlet, one alternate for each solenoid, this is the cheapest of valve types.
- **Proportional Valves**, which can regulate the flow of fluid or gas supplied to the actuator but with a higher cost than the previously mention valve;

- **Servo Valves**, by replacing the control solenoid in the proportional valves with servo motors it is possible for this valve to achieve faster actions with more precision but with much higher cost than the other mentioned valve types.

Directional valves were selected for the purpose of controlling the actuation of the pneumatic muscles due to their relatively low cost which is important when it is taken in to consideration that two valves are required for each muscle and several muscles for each finger.

To improve the controllability of the fingers additional flow control valves are placed in each fingers air supply so as to reduce the actuation speed of the finger according to the amplitude and force of the movement detected on each phalange of that particular finger. This valve will only influence the movement speed of the muscles of the finger it is responsible for reducing the number of proportional valves to 5 instead of the typical model of exclusive use of the same type that would require 20 valves per finger.

Calculating the specifications of the pneumatically actuated robotic system required some calculations into the air flow speed in pressurized conditions and how they could influence the performance stability in regards to how the controller would deal with changing speed parameters and nonlinearity.

The equation that provides the volume of air that passes thru a specific orifice per time interval is specified by equation (5.1) where T_a is the air temperature, it can be assumed room temperature of 25º, p_1 is the primary pressure, regulated in the air supply outlet which in the prototype operating condition is 400 kPa, p_2 is the secondary pressure, correspondent to the target vessel which is variable during pressurization and is dependent on each movement circumstance, d_o is the orifice diameter, the orifice of the valve is not circular but it is equivalent to a 2.11 diameter orifice, C is the discharge coefficient, for the valves used in the prototype it's 0.77383, F_γ is the specific heat ratio factor of the gas being pumped, in this case it is 1.4 for standard air, and x_T is the pressure differential factor, which is 0.72 in this case.

$$Q_a = \frac{1}{60} \cdot 4.17 \cdot C \cdot \left(\frac{d_o}{4.654}\right)^2 \cdot p_1 \cdot \left(1 - \frac{\frac{p_1 - p_2}{p_1}}{3 \cdot F_\gamma \cdot x_T}\right) \cdot \sqrt{\frac{\frac{p_1 - p_2}{p_1}}{T_a + 273.15}} \quad (5.1)$$

The initial air flow rate, with the target vessel at sea level pressure, is therefore 2.477 L/sec, and it is reduced significantly during pressurization of the pneumatic muscle due to the reduced pressure differential in relation to the source pressure, which is consider stable due to the pressure regulator on the pressurized tank.

In the test prototype a servo valve was constructed and controlled and then controlled by a Raspberry PI that changed the flow of air supplied to the directional control valves, improving the systems human following function by reducing the jerking impulses imposed by the air muscles when the pressure detected in the finger mechanism was small.

This type of proportional valve also improves the control valve life by reducing the on and off cycles.

Hand Mechanical Component

By assembling all the mechanical and actuation elements already described, we can render an approximation of the three dimensional model of the robotic exoskeleton glove, illustrated in figure 5.4. Different perspectives of the rendered robotic exoskeleton glove have been placed in appendix E.

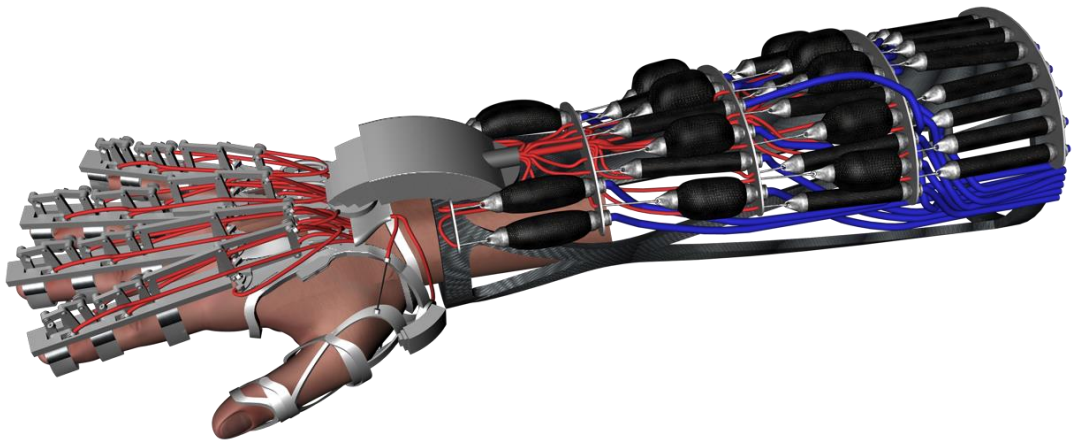

Fig 5.4: Rendering of the three dimensional model of the robotic exoskeleton glove

Over each finger articulation, there is a different joint mechanism dimensioned for that particular finger measurements. These mechanisms are actuated by two Bowden cables connected to two artificial muscles.

Every finger is attached to a rotating base on the hand support. This disc connector is also actuated in relation to the distance to its neighbour, or to the outside of the hand. The hand support is connected to the bracer through a semi-circular sliding mechanism with rotating base on each end to allow for flexion, extension and deviation of the wrist.

All Bowden cables are attached, either directly or indirectly, to an artificial muscle that pulls the inner cable, actuating the mechanism on the other end. Extension of the artificial muscle is performed by the contraction of the muscle responsible for the opposite movement of the same mechanism that the first actuator is connected to.

All the artificial muscles are attached to the bracer and are supplied with pressurised air with pneumatic tubes. This air supply is controlled by the flow and control valves that get their instruction from the microcontroller. The controlling electronics process the information collected from each sensor ring and determine the appropriate actuation, as well as record the list of input and output signals for future reproduction.

Critical analysis

The actuation system selected for this device proved, when tested, to perform better than the biological counterparts both in reaction time and in contraction force. By combining the actuation of independent finger joints with shared actuators and balancing the contraction of opposing muscles, it is possible to reduce the number of actuators, making it lighter and consequently more portable, without reducing the number of degrees of freedom already present on biological hands.

6

Control

Sensors

For the purpose of making the mechanism viable to be controller through both position and pressure, the sensor type selected was the strain gauge. This sensor changes its resistance proportionally to the deformation it is subjected to, when coupled to a flexible surface with a linear elastic modulus the deformation of the sensor will directly represent a defined pressure making it able to detect small finger displacements or to measure the force exerted by the user and transmit it to the system controller. The sensor also has additional benefits in its very small size, weight, cost and power requirements making it an efficient addition to the project.

The sensors were installed in an especially designed ring, illustrated in figure 6.1, that allow the user to control the pressure being applied by the robotic glove as well as controlling the fingers displacement thru a pressure balance of the strain gauge placed on the arch on top of the ring.

Fig 6.1: Rendering of the ring structure design to be used as position sensor

The arched carbon fibber on top of the ring is equipped with strain gauge inside and out on each side of the ring, this makes it possible to determine multidirectional movements, and another sensor beneath the finger to measure the pressure applied by the user on an object obstructing the fingers path.

In order to make the system compatible with slave class controllability and advanced mixed operation methods resistive linear motion encoders were installed in the actuators transition cables to determine the instant movement amplitude during independent operation. With this information and the pressure data collected by the strain gauge a central processing unit is able to record, reproduce and adjust the movements of the exoskeleton hand allowing the device more functionalities both as a robotic hand and an exoskeleton.

In the test prototype, due to limited manufacturing precision, the finger sensory structure was simplified so as to make it stronger, less prone to sensory errors and easier to tweak.

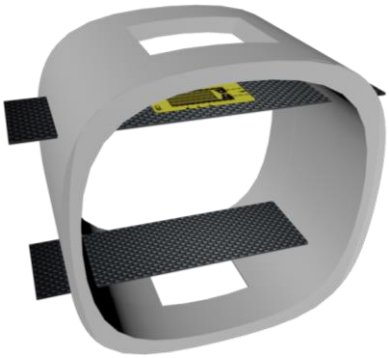

Fig 6.2: Rendering of the secondary ring structure used in the as position sensor

The test sensory ring, illustrated in figure 6.2, has only two strain gauge, one located on top and another in the bottom of the users' finger, this reduces the input the controller has to sort thru in order to identify the movement performed.

Tests made to the sensors in the prototype have proven to be very sensitive which results in constant small turbulence in sensory signals. This noise makes it necessary for larger amplitude detection signals, which means a slight increase in pressure form the users' finger to provide a distinct command to the controller. The fast actuation of the artificial muscles can also result in conflicting signals, when the user wants to close the finger but the mechanic contraction of the device exceeds the users' movement. This over actuation is solved in most cases thru the use of an actuated flow valve but the system still suffers from an occasional misinterpretation of the sensory command.

Instrumentation Amplifier

To amplify the measurements obtained from the strain gauge sensors and adjust their offset an instrumental amplifier was installed, illustrated in figure 6.3, between the sensor and the processing unit, enhancing the systems sensibility and making calibration easier.

The selected instrumentation amplifier, ilustrated in the schematic of figure 6.3, for the prototype was the INA826 from Texas Instruments which can amplify the input signal with a gain from 1 to 1000, adjustable with a resistor in the RG ports, and has all relevant constituents easily accessible from the chips ports so that the specifications can be adjusted acording to the systems requirements.

To improve the signal precision from the sensors, they were placed in a Wheatstone half-bridge. This circuit combines the opposing signals form the sensors to provide an average signal input and double the signal amplitude. In combination to the strain gauge, the half-bridge requires two more resistors to provide a reference for the sensor values. The ohmic value selected for these additional resistors is 5kΩ for each of them, this reduces the power dissipated in the circuit but maintains a sufficient current supply to the amplifier input.

In order to attain the largest signal amplitude, from the strain gauges in the Wheatstone half-bridge, the gain was calculated so that the output would be close to the maximum input of the controller. By using equation (6.1), we determined that, ideally, the gain must be 100, which means that, according to the gain obtained with equation (6.2), the resistance between RG terminals should be 499Ω, these equations were provided by the hardware documentation. Due to the additional components, mainly the potentiometer used to set the reference for the amplifier, identified as R8 in the schematic in figure 6.3, the resistance between RG had to be increased.

$$V_{out} = (V_{IN+} - V_{IN-}) \times G \tag{6.1}$$

$$G = 1 + \frac{49.4k\Omega}{RG} \tag{6.2}$$

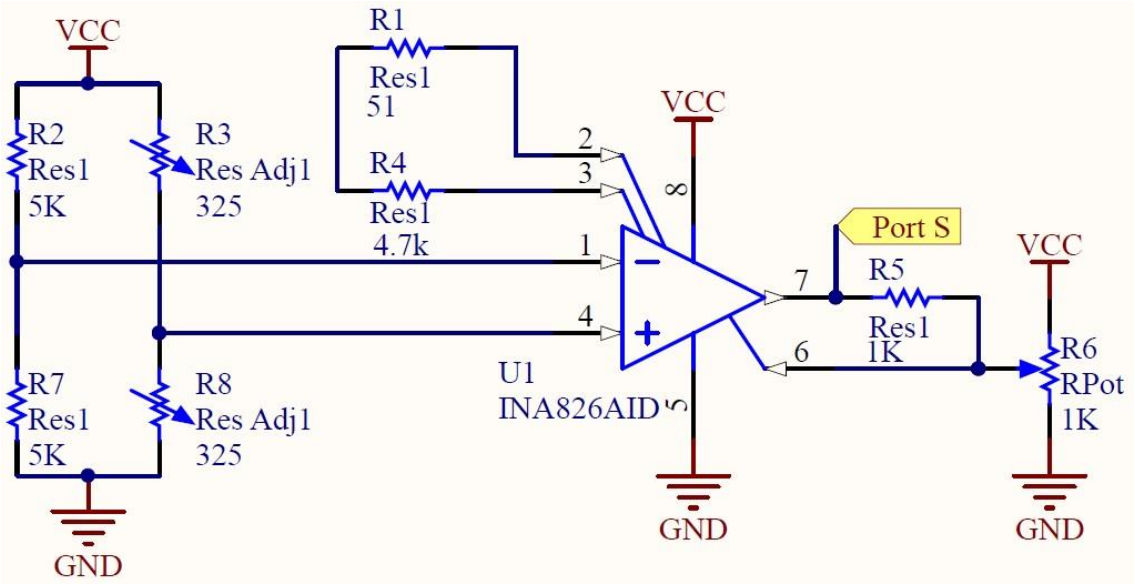

Fig 6.3: Diagram of the circuit implemented with the instrumentation amplifier

The strain gauge are represented in the circuit schematic by the R3 and R8 variable resistors, and along with R2 and R7, form a Wheatstone half-bridge whose terminals are connected to the input ports of the amplifier.

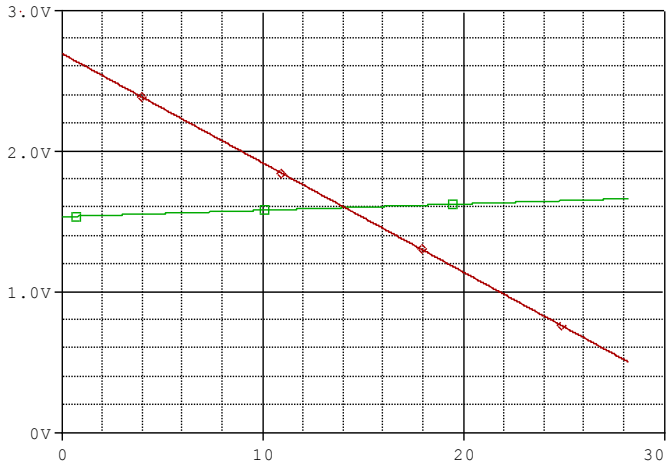

Fig 6.4: Amplification of the input signal in green into the output in red.

Figure 6.4 displays the simulation of the circuit ilustrated in figure 6.3. It is visible the rising input signal, in green, and compare its amplitude to the output, in red. The amplification is close to the expected in that it nearly reaches the supplied voltage, while avoiding signal saturation.

The reference of the amplifier is determined by a potenciometer. This alows for fine calibration of the sensory signal. During prototype testing, it was necessary to replace the resistor R3 with a variable resistor to alow for manual adjustments to be made to the gain resistance. This was necessary to rectify irregularities resulting from variations in component values, circuit cross interference and paricitic effects.

PIC

Control of the valve array is made with a series of dsPIC 33 microcontrollers[91], whose code is in appendix B, each of them dedicated to a pair of actuators reducing the parallel processing requirements, the schematic of the circuit with the microcontroller is illustrated on figure 6.5. These chips were selected based on their specifications, notably due to the fast processing speed and the 10 bit analogue to digital converters that result in fast and precise signal acquisition that further improve the sensing capabilities already refined in the acquired signal previous amplification and in the redundancy of the sensor installation.

The output signal to control the valves has to pass through mosfet power transistors to separate the 12V power supply required for the valve operation from the microcontroller 3.2V output signal.

The power supply for all the different electric systems included in the exoskeleton will have to be able to provide different voltages depending on the system being powered. Solenoid valves usually work with either 24V or 12V, for this project the latter was chosen, the microcontroller runs on less than 3.6V, this is the maximum voltage for the circuit, the working voltage for the prototype is 3.2V as indicated on V2 power supply in the schematic illustrated on figure 6.4, due to the specifications of the mosfet power transistors selected for this project, 5V were required to actuate them.

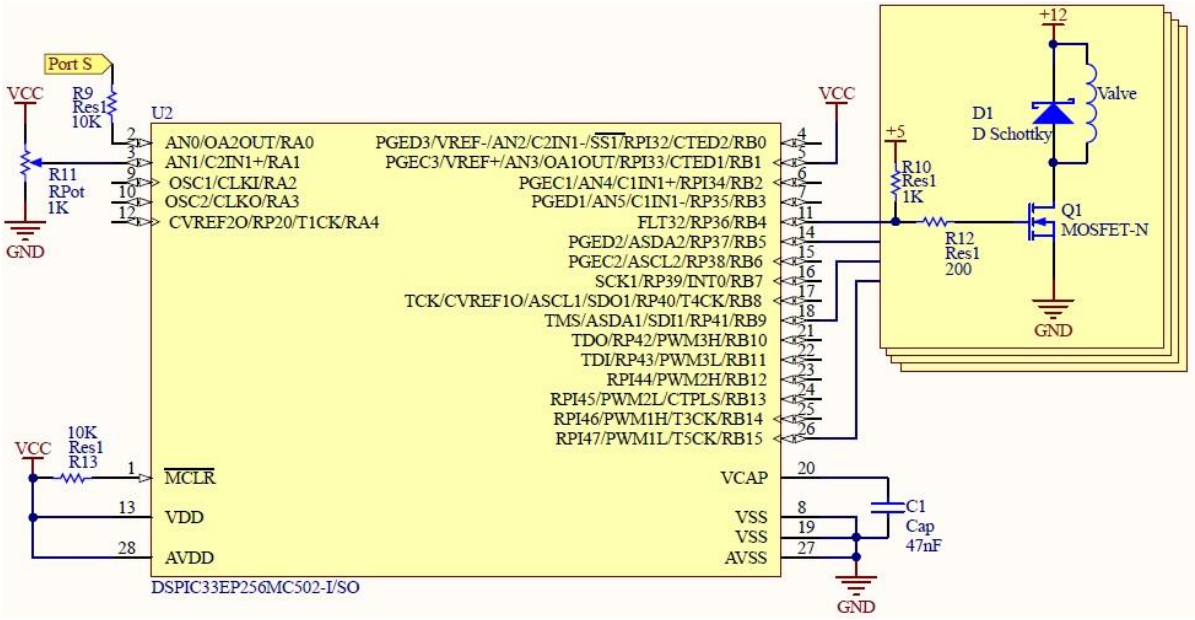

Fig 6.5: Diagram of the circuit implemented with the microcontroller

To increase the controllers performance each microcontroller will have be limited to controlling two pneumatic muscles, each of them requiring two solenoid valves, and one analogue signal input to be converted in to digital.

Each output port from the PIC has a step-up resistor to change the 3.2V signal in to the 5V the mosfet transistor requires to cross the gate threshold and activate the connected valve. All valves, labelled L1, L2, L3 and L4 in the circuit schematic, has a corresponding snubber diode to protect the transistor.

The analogue to digital converter of the chip takes in to consideration an adjustable input reference for the balanced measurement calculation. All signals under the reference are considered to be negative and as such are interpreted by the system as an indication as to which valves should be activated when the absolute amplitude of the converted signal surpasses the threshold.

Another controller was introduced in the development stage of the prototype, intended to provide the user with a numerical feedback of the sensory input of the device and control the custom servo valve constructed, for the purpose of perfecting the joint movement in small actuation amplitudes and increase the following precision of the mechanism. The additional processing unit used on the prototype was a raspberry pi and the code used to perform the required functions of display and control are in appendix C.

System Architecture

The control system architecture is divided into three main blocks, illustrated in figure 6.6. Starting with the information collection logic block where the sensors in the ring detect the finger pressure and send that information to the instrumentation amplifier.

Secondly, the control section is split in two parts. The left subsection applies a lower, faster and more direct control method that is performed by the dsPIC microcontroller[91], this is dedicated towards sensory measurement and muscle actuation. The subsection located on the right performs a higher control level, by making use of the Raspberry PI advanced capabilities it is able to run a machine learning algorithm on the recorded values from previous operations and control the actuation speed.

The final logic block is where the mechanical actuation is performed. The lowest control layer is responsible for opening and closing the air valves while the higher layer adjusts the air flow to the artificial muscles, slowing or hasting the operation of the actuator.

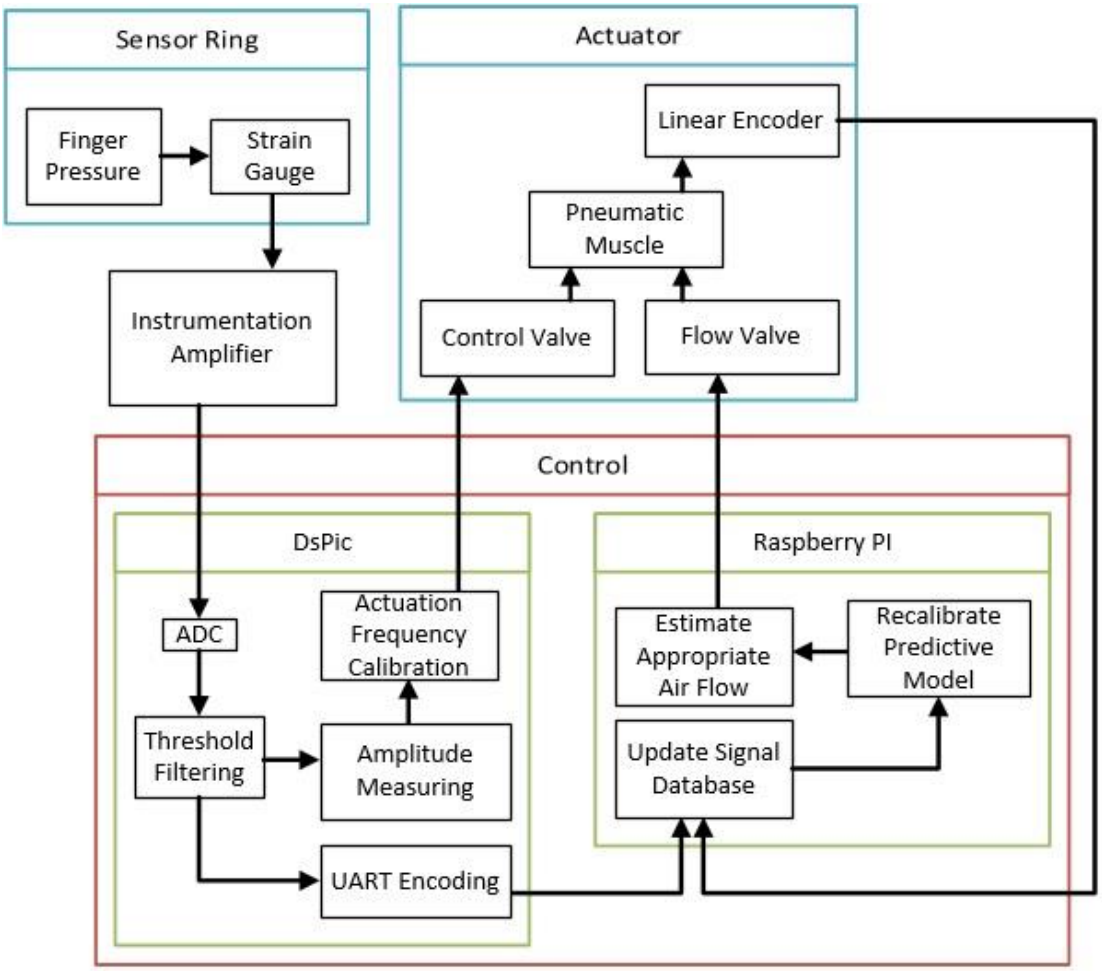

Fig 6.6: Conceptual Model representing the operation of the robotic hand.

Critical analysis

Controlling this robotic hand in the user following feature is sufficiently stable and precise although it requires some additional actuation control to differentiate muscle performance between fast and slow movements.

The central controlling unit, composed of a dsPIC and the surrounding circuitry, has more potential than was needed for this functionality. This microcontroller is able to take multiple samples of the signal provided by the strain gauge, apply a mean filter and transmit the measurement to a higher level processing unit while providing detection and actuation at a sufficient frequency for the process to remain imperceptible to the user.

The sensory system implemented in this project is significantly delicate and sensitive. It can easily break when overexerted, but by keeping that particularity in mind in the design of the sensor support it is easily safeguarded.

7

Conclusions and Future Works

General Conclusions

The device developed during this project demonstrated a viable alternative approach to the exoskeleton problem of hand robotic support and anthropomorphic gripers. With the analysis of the human biomechanical system many similarities to artificial mechanism were identified making it possible to apply the same strategies used by the human body to the robotic device.

Human muscles are constantly supplied by chemical energy that is released when it contracts in an identical way to the artificial pneumatic muscles and valves that are constantly supplied by energy in the form of pressurized gas that is released when an electrical signal is provided. Through experimental observation of different air muscles a length and volume was selected that differ from the anatomical distribution but it was required due to the fundamental differences between the organic and artificial muscles.

Bones of mammals have an intrinsic structure similar to composite materials making fabrics like carbon fibre ideal replacements for the external skeletal structure used in this artificial system. The frame of the exoskeleton had to be designed with the materials and ergonomic limitations in mind requiring the combination of structural and anatomical analysis to attain an architecture able to provide mechanical stability under linear and rotational forces while avoiding intersections with forearm muscles or other joints.

By studying the neural network of the human brain some conclusions were taken in regards to their similarity to the internal structure of micropro-

cessors where neurons work similarly to transistors but with more dynamic connections. Information and control signals inside the human body can also be compared to the electrical signals used in the robotic exoskeleton where the sensing and processing electronics use a lower electrical potential than the solenoid valves similarly to the electrochemical signals sent thru the body that are separated between faster dissipation of the sodium ions and long lasting calcium ions.

The mechanical articulation of the exoskeleton joints required a mathematical approach rather than a biologically inspired solution. To that purpose many previous exoskeleton gloves were studied to determine their approach to the problem and they were deemed lacking in either comfort or flexibility requiring that a new geometry be created.

Most of the objectives, indicated in the introduction chapter of the report, have been resolved throughout the different development sections.

In chapter 4, referring to the mechanical architecture of the device, the degrees of freedom of the hand were assured by separating each mechanical joint responsible for each finger articulation. Also in this chapter, the self-contained feature of the project was implemented through a support bracer able to comfortably hold all the actuators and control electronics required for this device.

In the fifth chapter the selected actuators were tested and shown to be faster and stronger than the human equivalent which satisfies the fourth requirement indicated in chapter 1.

The final system requirement, invisible control approach, was solved by the sixth chapter, dedicated to the control system, where an analysis of the sensor response revealed the signal instability which makes it necessary to slight change the expected human interaction. This change results in a need for a slight increase in finger pressure to positively identify a command signal but maintains a near invisible controllability of the device, sufficiently fulfilling the third requirement, invisible control approach.

A prototype of the finger mechanical joint was constructed with the respective control and actuation systems to serve has a proof of concept and allow for the controller to also be developed. The resulting system included the adjustable tension of the Bowden cables described in the air muscle support

and power management for transitioning between the processor and valves power requirements.

Future Work

Construction of a functional prototype of the entire exoskeleton glove will be required to develop the additional functioning envisioned for the project. This will be made easier with the advancements already provided mainly requiring the application of the described equations for the dimensions of each finger and the instalment of a joint in each articulation.

This device was dimensioned in such a way as to allow for integration in a modular full body exoskeleton, while focusing on the more detailed and less developed aspect of the robotic griper which has been overlooked in previous projects due to its complexity.

The power supply selected for this device also reflects the intent of being included into a full body exoskeleton by having a singular compressor supply a main pressures air tank that could provide the exoskeleton hands designed in this project as well as the actuators installed on the rest of the body.

References

[1] H. Yamaura, K. Matsushita, R. Kato, and H. Yokoi, 'Development of hand rehabilitation system for paralysis patient - universal design using wire-driven mechanism', *Conf. Proc. Annu. Int. Conf. IEEE Eng. Med. Biol. Soc. IEEE Eng. Med. Biol. Soc. Annu. Conf.*, vol. 2009, pp. 7122–7125, 2009.

[2] I. H. Ertas, E. Hocaoglu, D. E. Barkana, and V. Patoglu, 'Finger exoskeleton for treatment of tendon injuries', in *2009 IEEE International Conference on Rehabilitation Robotics*, 2009, pp. 194–201.

[3] A. Chiri *et al.*, 'HANDEXOS: Towards an exoskeleton device for the rehabilitation of the hand', in *2009 IEEE/RSJ International Conference on Intelligent Robots and Systems*, 2009, pp. 1106–1111.

[4] 'ExoHand'. [Online]. Available: https://www.festo.com/net/SupportPortal/Files/156734/Brosch_FC_ExoHand_EN_lo.pdf. [Accessed: 24-Oct-2016].

[5] 'Nuada'. [Online]. Available: http://nuada.pt/. [Accessed: 24-Oct-2016].

[6] 'Robotic Symbionts | Fluid Interfaces'. [Online]. Available: http://fluid.media.mit.edu/projects/robotic-symbionts. [Accessed: 24-Oct-2016].

[7] S. Nakagawara, H. Kajimoto, N. Kawakami, S. Tachi, and I. Kawabuchi, 'An Encounter-Type Multi-Fingered Master Hand Using Circuitous Joints', in *Proceedings of the 2005 IEEE International Conference on Robotics and Automation*, 2005, pp. 2667–2672.

[8] M. Fontana, A. Dettori, F. Salsedo, and M. Bergamasco, 'Mechanical design of a novel Hand Exoskeleton for accurate force displaying', 2009, pp. 1704–1709.

[9] 'deutschle cgi, CGI, 3D-Animation, Filmproduktion, CGI Stuttgart', *deutschle cgi, CGI, 3D-Animation, Filmproduktion, CGI Stuttgart*. [Online]. Available: http://www.deutschle.xyz/. [Accessed: 24-Oct-2016].

[10] ‘Shadow Dexterous Hand Technical Specification Shadow E1 Series’. .

[11] ‘Nuada.’ [Online]. Available: https://www.linkedin.com/company/nuada-lda. [Accessed: 24-Oct-2016].

[12] Digital Game Museum, *Neurosky Mindplay*. 2012.

[13] ‘Emotiv EPOC 14 Channel Mobile Neuroheadset Brain Computer Interface • CAD 329.97’, *PicClick CA*. [Online]. Available: http://picclick.ca/Emotiv-EPOC-14-Channel-Mobile-Neuroheadset-Brain-Computer-272337444886.html. [Accessed: 24-Oct-2016].

[14] M. Laurin, A. Canoville, and D. Germain, ‘Bone microanatomy and life-style: A descriptive approach’, *Comptes Rendus Palevol*, vol. 10, no. 5–6, pp. 381–402, Jul. 2011.

[15] B. says, ‘Periosteum Structure, Function; Periostitis, Periosteal Reaction | eHealthStar’. .

[16] G. H. Reference, ‘FGFR3 gene’, *Genetics Home Reference*. [Online]. Available: https://ghr.nlm.nih.gov/gene/FGFR3. [Accessed: 24-Oct-2016].

[17] N. Beyer Nardi and L. da Silva Meirelles, ‘Mesenchymal stem cells: isolation, in vitro expansion and characterization’, *Handb. Exp. Pharmacol.*, no. 174, pp. 249–282, 2006.

[18] T.-J. Lee *et al.*, ‘Enhancement of osteogenic and chondrogenic differentiation of human embryonic stem cells by mesodermal lineage induction with BMP-4 and FGF2 treatment’, *Biochem. Biophys. Res. Commun.*, vol. 430, no. 2, pp. 793–797, Jan. 2013.

[19] F. H. Netter and R. V. Dingle, *Musculoskeletal System: Anatomy, physiology and metabolic disorders*. Novartis Pharmaceuticals Corporation, 1997.

[20] ‘osteon | anatomy | Britannica.com’. [Online]. Available: https://www.britannica.com/science/osteon. [Accessed: 24-Oct-2016].

[21] ‘general-osteology-13-638.jpg (JPEG Image, 638 × 479 pixels) - Scaled (80%)’. [Online]. Available: http://image.slidesharecdn.com/generalosteology-130128111649-phpapp01/95/general-osteology-13-638.jpg?cb=1359371951. [Accessed: 24-Oct-2016].

[22] C. M. Gdyczynski, A. Manbachi, S. Hashemi, B. Lashkari, and R. S. C. Cobbold, ‘On estimating the directionality distribution in pedicle trabecular bone from micro-CT images’, *Physiol. Meas.*, vol. 35, no. 12, pp. 2415–2428, Dec. 2014.

[23] pmhdev, ‘Endosteum - National Library of Medicine’, *PubMed Health*. [Online]. Available: https://www.ncbi.nlm.nih.gov/pubmedhealth/PMHT0027353/. [Accessed: 24-Oct-2016].

[24] F. Levrero-Florencio, L. Margetts, E. Sales, S. Xie, K. Manda, and P. Pankaj, 'Evaluating the macroscopic yield behaviour of trabecular bone using a nonlinear homogenisation approach', *J. Mech. Behav. Biomed. Mater.*, vol. 61, pp. 384–396, Aug. 2016.

[25] 'Articular Cartilage - Wheeless' Textbook of Orthopaedics'. [Online]. Available: http://www.wheelessonline.com/ortho/articular_cartilage. [Accessed: 24-Oct-2016].

[26] B. L. Schumacher, J. A. Block, T. M. Schmid, M. B. Aydelotte, and K. E. Kuettner, 'A novel proteoglycan synthesized and secreted by chondrocytes of the superficial zone of articular cartilage', *Arch. Biochem. Biophys.*, vol. 311, no. 1, pp. 144–152, May 1994.

[27] 'Bone Tissue Composition Chapter 6. Bone Textures Compact bone – Dense outer layer Spongy (cancellous) bone – Honeycomb of trabeculae found at the bone. - ppt download'. [Online]. Available: http://slideplayer.com/slide/9806326/. [Accessed: 24-Oct-2016].

[28] C. D. Clemente, *Anatomy: A Regional Atlas of the Human Body*, 6 edition. Philadelphia: LWW, 2010.

[29] 'Mark Gardner Gibson | Animatronic Arm | Forearm Design'. [Online]. Available: http://www.markgardnergibson.com/projects/robotarm/forearm/index.shtml. [Accessed: 24-Oct-2016].

[30] B. Kingston, *Understanding Joints: A Practical Guide to Their Structure and Function*. Nelson Thornes, 2000.

[31] 'Bones of the Hand: Carpals, Metacarpals and Phalanges', *TeachMeAnatomy*, 17-Apr-2012. .

[32] R. W. Beasley, *Beasley's Surgery of the Hand*. Thieme, 2003.

[33] R. Tubiana, J.-M. Thomine, and E. Mackin, *Examination of the Hand and Wrist*. CRC Press, 1998.

[34] 'Osteology Flashcards - Biological Anthropology 2414 with Cunningham at Texas State University-San Marcos - StudyBlue'. [Online]. Available: https://www.studyblue.com/notes/note/n/osteology-flashcards/deck/16758604. [Accessed: 24-Oct-2016].

[35] H. Gray, *Anatomy of the Human Body*. Lea & Febiger, 1918.

[36] 'My Site'. [Online]. Available: http://importanceoftheskeletalsystem.weebly.com/. [Accessed: 24-Oct-2016].

[37] 'Size of Apical Phalangeal Tufts | CARTA'. [Online]. Available: https://carta.anthropogeny.org/moca/topics/apical-phalangeal-tufts. [Accessed: 24-Oct-2016].

[38] A. Sandow, 'Excitation-Contraction Coupling in Muscular Response', *Yale J. Biol. Med.*, vol. 25, no. 3, pp. 176–201, Dec. 1952.

[39] V. P. Eroschenko, *diFiore's Atlas of Histology: with Functional Correlations*, 12 edition. Philadelphia: LWW, 2012.

[40] S. R. Goodman, *Medical Cell Biology*, 3rd edition. Academic Press, 2007.

[41] 'The Muscular System'. [Online]. Available: http://classes.midlandstech.edu/carterp/Courses/bio110/chap07/chap07.html. [Accessed: 24-Oct-2016].

[42] D. Purves *et al.*, 'Neuroscience', 2001.

[43] T. O. McCracken, Ed., *The New Atlas of Human Anatomy*, 3rd edition. London: Constable, 2001.

[44] 'Muscles at Northern Arizona University', *StudyBlue*. [Online]. Available: https://www.studyblue.com/notes/note/n/muscles/deck/15714078. [Accessed: 24-Oct-2016].

[45] L. R. Otterbein, P. Graceffa, and R. Dominguez, 'The crystal structure of uncomplexed actin in the ADP state', *Science*, vol. 293, no. 5530, pp. 708–711, Jul. 2001.

[46] M. J. Tyska and D. M. Warshaw, 'The myosin power stroke', *Cell Motil. Cytoskeleton*, vol. 51, no. 1, pp. 1–15, Jan. 2002.

[47] S. Labeit and B. Kolmerer, 'Titins: giant proteins in charge of muscle ultrastructure and elasticity', *Science*, vol. 270, no. 5234, pp. 293–296, Oct. 1995.

[48] J. R. Knowles, 'Enzyme-catalyzed phosphoryl transfer reactions', *Annu. Rev. Biochem.*, vol. 49, pp. 877–919, 1980.

[49] A. F. Huxley and R. Niedergerke, 'Structural changes in muscle during contraction; interference microscopy of living muscle fibres', *Nature*, vol. 173, no. 4412, pp. 971–973, May 1954.

[50] I. M. Robertson, Y.-B. Sun, M. X. Li, and B. D. Sykes, 'A structural and functional perspective into the mechanism of Ca2+-sensitizers that target the cardiac troponin complex', *J. Mol. Cell. Cardiol.*, vol. 49, no. 6, pp. 1031–1041, Dec. 2010.

[51] E. R. Kandel, J. H. Schwartz, T. M. Jessell, S. A. Siegelbaum, and A. J. Hudspeth, Eds., *Principles of Neural Science.*, 5th edition. New York: McGraw-Hill Education / Medical, 2012.

[52] L. G. JOZSA and P. Kannus, *Human Tendons: Anatomy, Physiology and Pathology*. Champaign, Illinois: Human Kinetics |The Journal of Bone & Joint Surgery, 1997.

[53] 'Myotendinous Junction - Cellular Development, Function & Anatomy - LifeMap Discovery'. [Online]. Available: http://discovery.lifemapsc.com/IN-VIVO-DEVELOPMENT/TENDON-LIGAMENT/MYOTENDINOUS-JUNCTION. [Accessed: 24-Oct-2016].

[54] J.-C. Guimberteau, J.-P. Delage, and J. Wong, 'The role and mechanical behavior of the connective tissue in tendon sliding', *Chir. Main*, vol. 29, no. 3, pp. 155–166, Jun. 2010.

[55] A. Biswas, M. Manivannan, and M. A. Srinivasan, 'Vibrotactile sensitivity threshold: nonlinear stochastic mechanotransduction model of the Pacinian Corpuscle', *IEEE Trans. Haptics*, vol. 8, no. 1, pp. 102–113, Mar. 2015.

[56] E. Kandel, J. Schwartz, and T. Jessell, *Principles of Neural Science*, 4th edition. McGraw-Hill Companies, Incorporated, 2000.

[57] 'Baby's Brain Begins Now: Conception to Age 3'. [Online]. Available: http://www.urbanchildinstitute.org/why-0-3/baby-and-brain. [Accessed: 24-Oct-2016].

[58] 'SD3Control'. [Online]. Available: http://mcqs.leedsmedics.org.uk/Year%202/C&MT2/SD3ControlMC.html. [Accessed: 24-Oct-2016].

[59] E. D. Adrian and K. Umrath, 'The impulse discharge from the pacinian corpuscle', *J. Physiol.*, vol. 68, no. 2, pp. 139–154, Oct. 1929.

[60] M. Paré, R. Elde, J. E. Mazurkiewicz, A. M. Smith, and F. L. Rice, *The Meissner Corpuscle Revised: A Multiafferented Mechanoreceptor with Nociceptor Immunochemical Properties*. 2000.

[61] K. E. Barrett, S. M. Barman, S. Boitano, and H. L. Brooks, *Ganong's Review of Medical Physiology, 23rd Edition*, 23 edition. New York: McGraw-Hill Medical, 2009.

[62] S. M. Sherman and R. W. Guillery, *Exploring the Thalamus*. Elsevier, 2001.

[63] K. T. Patton, *Anatomy and Physiology*. Elsevier Health Sciences, 2015.

[64] 'Tickle And Itch - Medical Physiology - Euroform Healthcare'. [Online]. Available: http://www.euroformhealthcare.biz/medical-physiology/tickle-and-itch.html. [Accessed: 24-Oct-2016].

[65] 'Parietal Lobe'. [Online]. Available: http://www.ruf.rice.edu/~lngbrain/cglidden/parietal.html. [Accessed: 14-Sep-2016].

[66] W. Penfield and E. Boldrey, 'Somatic motor and sensory representation in the cerebral cortex of man as studied by electrical stimulation', *Brain J. Neurol.*, vol. 60, pp. 389–443, 1937.

[67] 'Anatomy', *Pinterest*. [Online]. Available: https://www.pinterest.com/pin/162411130285017021/. [Accessed: 24-Oct-2016].

[68] C.-B. Rivara, C. C. Sherwood, C. Bouras, and P. R. Hof, 'Stereologic characterization and spatial distribution patterns of Betz cells in the human primary motor cortex', *Anat. Rec. A. Discov. Mol. Cell. Evol. Biol.*, vol. 270A, no. 2, pp. 137–151, Feb. 2003.

[69] S. L. Palmer, S. C. Noctor, B. Jablonska, and S. L. Juliano, 'Laminar specific alterations of thalamocortical projections in organotypic cultures following layer 4 disruption in ferret somatosensory cortex', *Eur. J. Neurosci.*, vol. 13, no. 8, pp. 1559–1571, Apr. 2001.

[70] D. Mysid, 'A simplified view of an artifical neural network.', 28-Nov-2006. [Online]. Available: https://commons.wikimedia.org/wiki/File:Neural_network.svg. [Accessed: 24-Oct-2016].

[71] 'AlanTuring.net Turing's Neural Networks'. [Online]. Available: http://www.alanturing.net/turing_archive/pages/reference%20articles/connectionism/Turing's%20neural%20networks.html. [Accessed: 24-Oct-2016].

[72] K. H. Levin, *Comprehensive Clinical Neurophysiology*. W.B. Saunders, 2000.

[73] 'Temporal Summation'. [Online]. Available: http://lecerveau.mcgill.ca/flash/capsules/articles_pdf/temporal_summation.pdf. [Accessed: 25-Oct-2016].

[74] 'Intrinsic Muscles of the Hand - Wheeless' Textbook of Orthopaedics'. [Online]. Available: http://www.wheelessonline.com/ortho/intrinsic_muscles_of_the_hand. [Accessed: 25-Oct-2016].

[75] M. Schünke, L. M. Ross, E. Schulte, U. Schumacher, and E. D. Lamperti, *Thieme Atlas of Anatomy: General Anatomy and Musculoskeletal System*. Thieme, 2006.

[76] 'Muscles of the Hand', *TeachMeAnatomy*, 03-Jun-2012. [Online]. Available: http://teachmeanatomy.info/upper-limb/muscles/hand/. [Accessed: 24-Oct-2016].

[77] M. Inc, *Mosby's Medical Dictionary*. Mosby/Elsevier, 2009.

[78] H. Gray, *Anatomy: descriptive and surgical*, 1st ed. London: J.W. Parker, 1858.

[79] N. Palastanga and R. Soames, *Anatomy and Human Movement: Structure and Function*. Churchill Livingstone/Elsevier, 2012.

[80] 'Hand therapy', *Pinterest*. [Online]. Available: https://www.pinterest.com/jomi100/hand-therapy/. [Accessed: 24-Oct-2016].

[81] J. A. Gosling, P. F. Harris, J. R. Humpherson, I. Whitmore, and P. L. T. Willan, *Human Anatomy: Color Atlas and Textbook*, 5th edition. Edinburgh? Elsevier, 2008.

[82] 'A&P Exam 2 at Loyola University Chicago', *StudyBlue*. [Online]. Available: https://www.studyblue.com/notes/note/n/a-p-exam-2/deck/14192991. [Accessed: 24-Oct-2016].

[83] K. L. Moore and A. M. R. Agur, *Essential Clinical Anatomy*. Lippincott Williams & Wilkins, 2007.

[84] W. Platzer, *Color Atlas and Textbook of Human Anatomy: Locomotor system*. Thieme, 2004.

[85] K. F. Lutsky, E. L. Giang, and J. L. Matzon, 'Flexor Tendon Injury, Repair and Rehabilitation', *Orthop. Clin. North Am.*, vol. 46, no. 1, pp. 67–76, Jan. 2015.

[86] P. K. Levangie and C. C. Norkin, *Joint Structure and Function: A Comprehensive Analysis*. F.A. Davis, 2011.

[87] H. V. Carter, H. Gray, and S. this Book, *superficial muscles of back of forearm*. 1858.

[88] G. H. Baek, J. S. Kim, and M. S. Chung, 'Isolated ischemic contracture of the mobile wad: a report of two cases', *J. Hand Surg. Edinb. Scotl.*, vol. 29, no. 5, pp. 508–509, Oct. 2004.

[89] 'Muscles of the Arm and the Hand - anatomical plates.' [Online]. Available: http://www.corpshumain.ca/en/muscle_bras_en.php. [Accessed: 27-Oct-2016].

[90] 'REFLEXOLOGY TO INDUCE LABOUR - Reflexology-map.com', *Reflexology Map | food reflexology chart | hand pressure points*, 06-Apr-2015. .

[91] 'dsPIC33EPXXXMC20X/50X Data Sheet - 70000657H.pdf'. [Online]. Available: http://ww1.microchip.com/downloads/en/DeviceDoc/70000657H.pdf. [Accessed: 15-Oct-2016].

APPENDICES

Appendix A.1

MATLAB Algorithm to calculate the dimensions of the mechanical joints as described in Figure 4.2.

```
clear all, close all
clc

global R;
% R : Distance from remote centre of rotation to the attachment base
R=2;
Mi=0;
% Configuration of the particle swarm optimization algorithm
options=optimoptions('particleswarm','SwarmSize',600,'Display', 'iter','MaxIter',600,'SelfAdjustment',2,'SocialAdjustment',2,'HybridFcn',@fmincon);

% Upper and Lower Boundaries of each z(x) value
lb=[0.1,0.01,0.01,0,0];
ub=[4,1,5,pi()/2,1];
rng default
z=particleswarm(@fiting_5,5, lb,ub, options)

% z(1) : Available length of the attachment base on the finger
% z(2) : Proportion of the base reserved for vector A
% z(3) : Length of C in relation to B
% z(4) : Angle zeta located between C and B and measured from alpha to base
% z(5) : Distance between axis CE and the base

A=z(1)*z(2);
B=A+R;
```

```
C=B*z(3);
E=z(1)-A;
zeta=z(4);
G=z(5);
alpha=ones(91,1)*acos(A/B);
D=sqrt((sin(alpha(1))*B+sin(alpha(1)-zeta)*C-G)^2+(cos(alpha(1)-zeta)*C-
A-E)^2);

M=0;
Re=0;
% Repeat calculations for each angle of the remote centre of rotation from
0º to 90º
for k=0:+1:90
   % Calculate the value of the angle alpha
   alpha(k+1)= abs(acos((A+tan((k/180*pi())/2)*R)/(A+R)));
   % Calculate the distance between the axis BC and DE
   hip=sqrt((sin(alpha(k+1))*B-G)^2+(cos(alpha(k+1))*B+E)^2);
   % Calculate the angle of the axis of DE
   teta=acos((D^2+hip^2-C^2)/(2*D*hip))+acos((E^2+hip^2-(B-
G/sin(alpha(k+1)))^2)/(2*E*hip));
   % Calculate the angle of the axis of CD
   beta=acos((D^2+C^2-hip^2)/(2*D*C));
   % Calculate the angle of the axis of BC In relation to the horizontal line
   gama=(acos((hip^2+C^2-D^2)/(2*hip*C))+acos((hip^2+B^2-
(G^2+E^2))/(2*hip*B))-alpha(k+1));
   % Calculation of the horizontal displacement of edge B in relation to the
remote centre of rotation
   x=abs(cos(gama+zeta)*B+tan((k/180*pi())/2)*R-cos(gama+zeta-
alpha(k+1))*A);
   % Calculation of the vertical displacement of edge B in relation to the
remote centre of rotation
   y=abs(R+(sin(alpha(k+1))-sin(gama+zeta))*B+sin(gama+zeta-
alpha(k+1))*A);
   % Calculation of the height of the CD axis relative to the base
   Mi(k+1)=abs(sin(teta)*D+G);
   % Remote rotation centre error vector
   e(k+1)=abs(R-abs(sqrt(x^2+y^2)));
   % Sum of accumulated error
   Re=Re+(e(k+1))^2;
end
% Mean of mismatch
erro=real(Re/91);

% Representation of the error observed during the joint rotation
figure(1)
plot(0:90,e,'y');
```

```
% Representation of the value of alpha angle during the joint rotation
figure(2)
plot(0:90, alpha*(180/pi()), 'r',0:90, 90:-1:0, 'b');
% Representation of the error during the joint rotation
figure(3)
plot(0:90, Mi,'g');
```

Appendix A.2

MATLAB Function used by the swarm algorithm to optimize the geometric dimensions of Figure 4.2.

```
function [ erro ] = fiting_5( z )

% R : Distance from remote centre of rotation to the attachment base
global R;

% z(1) : Available length of the attachment base on the finger
% z(2) : Proportion of the base reserved for vector A
% z(3) : Length of C in relation to B
% z(4) : Angle zeta located between C and B and measured from alpha to base
% z(5) : Distance between axis CE and the base

A=z(1)*z(2);
B=A+R;
C=B*z(3);
E=z(1)-A;
zeta=z(4);
G=z(5);
alpha=acos(A/B);
D=sqrt((sin(alpha)*B+sin(alpha-zeta)*C-G)^2+(cos(alpha-zeta)*C-A-E)^2);

M=0;
Re=0;
% Repeat calculations for each angle of the remote centre of rotation from 0º to 90º
for k=0:+1:90
   % Calculate the value of the angle alpha
   alpha= abs(acos((A+tan((k/180*pi())/2)*R)/(A+R)));
   % Calculate the distance between the axis BC and DE
   hip=sqrt((sin(alpha)*B-G)^2+(cos(alpha)*B+E)^2);
   % Calculate the angle of the axis of DE
   teta=acos((D^2+hip^2-C^2)/(2*D*hip))+acos((E^2+hip^2-(B-G/sin(alpha))^2)/(2*E*hip));
   % Calculate the angle of the axis of CD
   beta=acos((D^2+C^2-hip^2)/(2*D*C));
   % Calculate the angle of the axis of BC In relation to the horizontal line
   gama=(acos((hip^2+C^2-D^2)/(2*hip*C))+acos((hip^2+B^2-(G^2+E^2))/(2*hip*B))-alpha);
   % Calculation of the horizontal displacement of edge B in relation to the remote centre of rotation
```

```
        x=abs(cos(gama+zeta)*B+tan((k/180*pi())/2)*R-cos(gama+zeta-
alpha)*A);
        % Calculation of the vertical displacement of edge B in relation to the
remote centre of rotation
        y=abs(R+(sin(alpha)-sin(gama+zeta))*B+sin(gama+zeta-alpha)*A);
        % Calculation of the height of the CD axis relative to the base
        M=M+abs(sin(teta)*D+G);
        % Remote rotation center error vector
        e(k+1)=abs(R-abs(sqrt(x^2+y^2)));
        % Sum of accumulated error
        Re=Re+(e(k+1))^2;
    end
    % Maximum error calculated in the joint movement with adjusted weight
    erro=real(1000*max(e));
    end
```

Appendix B.1

Microcontroller main code

```
#include <stdio.h>
#include <p33EP256MC202.h>
#include <math.h>
#include <dsp.h>
#include <stdlib.h>
#include "mcc_generated_files/mcc.h"

// Minimum Actuation threshold
#define Min_Act     30
// Minimum stoping threshold
#define Min_Stop     15
// Offset for the measured sensory amplitude
#define referencia 0
// Delay scale for communication interval
#define DELAY 1

// Function prototypes
void setup_valve();
void mover(signed int Amplitude);
void parar();

int main(void)   {
   // Initialization of the internal parameters of the system
   SYSTEM_Initialize();
   // Initializing the timer
   T1CON = 0x8030;
   // Initiation of the parameters of the output signals
   setup_valve();
   // Auxiliar variable to read the sensory input
   signed int aux1;
   // Variable dimensioned for the uart package size
   uint8_t num_write;

   // Cycle of operation of the joint controlling chip
   while (1) {
      // Reading of the analogue signal from the sensor
      aux1 = (signed int) ADC1BUF0 - referencia;
      // Conversion of the 9-bit sensory signal plus polarity in to a signal
to byte value
      num_write=(abs(aux1)-1)/2;
      // Sending signal amplitude to the advanced processing platform
      UART1_Write( num_write);
```

```
            // Reset timer
            TMR1 = 0;
            // Sending the sensory signal to the actuation function
            mover(aux1);
            // Delay between sensory signal processing
            while (TMR1 < DELAY*512){}
        }
        return 0;
    }

    // Signal evaluation function to identify whether the actuation or stop threshold
    // has been reached and, if the first is confirmed, which valves shall be actuated
    void mover(signed int Amplitude) {

        // Verification of actuation threshold
        if (abs(Amplitude) >= Min_Act) {
            if (Amplitude > 0) {    // Selecting the directionality of positive actuation
                TRISBbits.TRISB9 = 1;
                TRISBbits.TRISB15 = 1;
                TRISBbits.TRISB4 = 0;
                TRISBbits.TRISB5 = 0;
            } else {    // Selecting the directionality of the negative actuation
                TRISBbits.TRISB4 = 1;
                TRISBbits.TRISB5 = 1;
                TRISBbits.TRISB9 = 0;
                TRISBbits.TRISB15 = 0;
            }
        }
        // Detection of valve closing threshold
        if ((abs(Amplitude) <= Min_Stop)) {
            parar();
        }
    }

    // Function responsible for closing all valves
    void parar() {
        TRISBbits.TRISB4 = 0;
        TRISBbits.TRISB5 = 0;
        TRISBbits.TRISB9 = 0;
        TRISBbits.TRISB15 = 0;
    }

    // Output setup for valve control
```

```
void setup_valve(){
   // Set Input Pins
   TRISAbits.TRISA0 = 1;
   TRISAbits.TRISA1 = 1;

   // OPEN-DRAIN CONFIGURATION
   ODCBbits.ODCB4 = 1;
   ODCBbits.ODCB5 = 1;
   ODCBbits.ODCB9 = 1;
   ODCBbits.ODCB15 = 1;

   // Set output ports as closed
   TRISBbits.TRISB4 = 0;
   TRISBbits.TRISB5 = 0;
   TRISBbits.TRISB9 = 0;
   TRISBbits.TRISB15 = 0;
}
```

Appendix B.2

Microcontroller configuration tables

System Module	
FGS	0X3
FICD	0X3
FOSC	0X43
FOSCSEL	0X40
FPOR	0X60
FWDT	0X7F
Internal Oscilator	
CLKDIV	0X3100
CORCON	0X0
OSCCON	0X0
OSCTUN	0X0
PLLFBD	0X32
RCON	0X0
REFOCON	0X0
RESET	
RCON	0X0

PIN MODULE			
ANSELA	0X13	RPINR18	0X26
ANSELB	0X103	RPINR19	0X0
CNENA	0X0	RPINR22	0X0
CNENB	0X0	RPINR23	0X0
CNPDA	0X0	RPINR26	0X0
CNPDB	0X0	RPINR3	0X0
CNPUA	0X0	RPINR37	0X0
CNPUB	0X0	RPINR38	0X0
LATA	0X0	RPINR39	0X0
LATB	0X80	RPINR7	0X0
ODCA	0X0	RPINR8	0X0
ODCB	0X0	RPOR0	0X0
RPINR0	0X0	RPOR1	0X0
RPINR1	0X0	RPOR2	0X100
RPINR11	0X0	RPOR3	0X0
RPINR12	0X0	RPOR4	0X0
RPINR14	0X0	TRISA	0X1F
RPINR15	0X0	TRISB	0XFF7F

ADC1	
AD1CHS0	0X100
AD1CHS123	0X0
AD1CON1	0X81E4
AD1CON2	0X4
AD1CON3	0X4
AD1CON4	0X0
AD1CSSH	0X0
AD1CSSL	0X0

UART1	
U1BRG	0X5F
U1MODE	0X8008
U1STA	0X0
U1TSREG	0X0

Appendix C

C code used in the Raspberry PI controller for acquiring data transmitted from the microcontroller via UART and provide the signal to control the proportional valve.

```
#include <stdlib.h>
#include <stdio.h>
#include <fcntl.h>
#include <sys/mman.h>
#include <unistd.h>

#include "rs232.h"
#include <time.h>

#include <wiringPi.h>

// Define GPIO pin numbers
const int pol_pin = 17;
const int dir_pin = 27;
const int ena_pin = 22;
// Define percision margin
const int margem = 75;
// Define input amplitude to signal output scale
const int escala = 25;
// Define read delay
const int ler_delay = 100;
// Define output signal interval
const int enviar_delay = 100;

int main() {
 // Setup GPIO pins
 wiringPiSetupGpio();

 int n,                  /* Number of bytes read */
    cport_nr=16,         /* /dev/ttyUSB0 (n.a. on windows) */
    bdrate=9600;         /* 9600 baudrate */
    abertura = 1;        /* Proportional valve opening*/
    pol_on = 0;          /* Impulse state, on = 1 and off = 0 */
 // Direction of valve actuation, open or close
 signed int dir = 1;
 // Input signal
 unsigned char buff[2];
 // RS232 operation parameters
```

```
        char mode[]={'8','N','1',0};
        // Configure GPIO output pins
        pinMode(pol_pin, OUTPUT);
        pinMode(dir_pin, OUTPUT);
        pinMode(ena_pin, OUTPUT);

        if(RS232_OpenComport(cport_nr, bdrate, mode)) { // Error if unable to
connect RS232 adapter
          printf("Cannot open comport\n");
          return(0);
        }
        // Set enable pin as off, GPIO in active low
        digitalWrite(ena_pin, HIGH);
        // Setup read and write clock timers
        clock_t tempo_ler = clock();
        clock_t tempo_enviar = clock();

        while(1) {
          if (clock() >= (tempo_ler + ler_delay)) {
            // Reset read timer
            tempo_ler = clock();
            // Read input signal
            n = RS232_PollComport(cport_nr, buff, 1);
            if(n > 0) {  // Print the read signal
              sinal = buff[0]* escala;
              // If signal bigger than current opening then close the valve
              if ((buff[0] * escala) > (abertura + margem)) {
                dir = 1;
                digitalWrite(dir_pin, LOW);
                digitalWrite(ena_pin, LOW);
                printf("on  up  ");
              } else if ((buff[0] * escala) < (abertura - margem)) {  // If signal smaller
than current opening then open the valve
                dir = -1;
                digitalWrite(dir_pin, HIGH);
                digitalWrite(ena_pin, LOW);
                printf("on down ");
              } else {  // If signal is within the margin of error then stop valve
movement
                dir = 0;
                digitalWrite(ena_pin, HIGH);
                printf("off     ");
              }
              printf("received bytes: %d", buff[0]);
              printf("    Opening amplitude: %d\n", abertura);
            }
```

```
    }
    // Square signal construction
    if (clock() >= (tempo_enviar + enviar_delay {
      // Reset signal timer
      tempo_enviar = clock();
      if ((sinal < (abertura - margem)) || (sinal > (abertura + margem))) {
        // increase or decrease valve opening
        abertura = abertura + dir;
        // if previous signal wave is high then change to low
        if (pol_on == 1) {
          digitalWrite(pol_pin, LOW);
          pol_on = 0;
        } else {  // if previous signal wave is low then change to high
          digitalWrite(pol_pin, HIGH);
          pol_on = 1;
        }
      }
    }
  }
  return(0);
}
```

Appendix D

	Length of the muscle mechanism (cm)			
Weight (g)	2 Bar	3 Bar	4 Bar	5 Bar
900	20.1	19.75	19.3	18.9
1100	20.3	19.8	19.4	19
1300	20.4	19.8	19.45	19.1
1500	20.5	19.8	19.45	19.2
1700	20.6	19.8	19.5	19.2
1900	20.6	19.9	19.5	19.2
2100	20.65	19.9	19.6	19.25
2300	20.7	20	19.6	19.4
2500	20.8	20	19.7	19.4
2700	20.8	20.1	19.7	19.5
2900	20.9	20.1	19.75	19.4
3100	21	20.2	19.8	19.4
3300	21	20.25	19.8	19.4
3500	21.1	20.3	19.9	19.45
3700	21.2	20.4	19.9	19.5
3900	21.3	20.45	19.95	19.6
4100	21.35	20.45	19.9	19.5
4300	21.4	20.5	20	19.7
4500	21.4	20.5	20	19.65
4700	21.5	20.6	20	19.8
4900	21.6	20.7	20.1	19.8
5100	21.6	20.85	20.2	19.9
5300	21.7	20.8	20.2	19.95
5500	21.7	20.9	20.2	19.9
5700	21.8	20.9	20.2	19.95
5900	21.8	21	20.2	20
6100	21.9	21	20.3	19.95
6300	21.9	21.05	20.4	20.05
6500	22	21	20.45	20.1
6700	22.15	21.05	20.5	20.15
6900	22.2	21.2	20.5	20.2

Appendix E

Different perspectives of the rendered robotic exoskeleton glove.

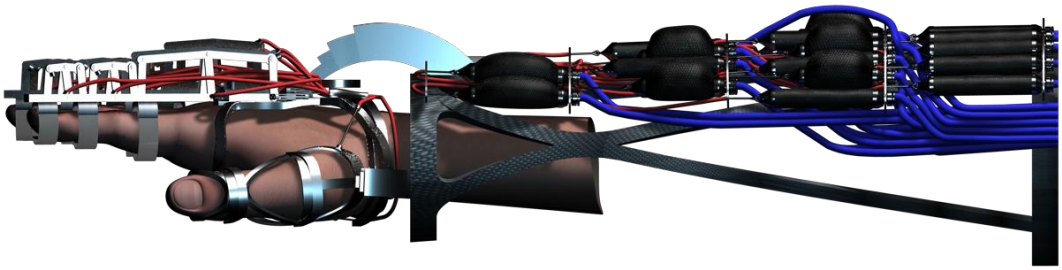

Fig 8.1: Left perspective of the rendered robotic glove

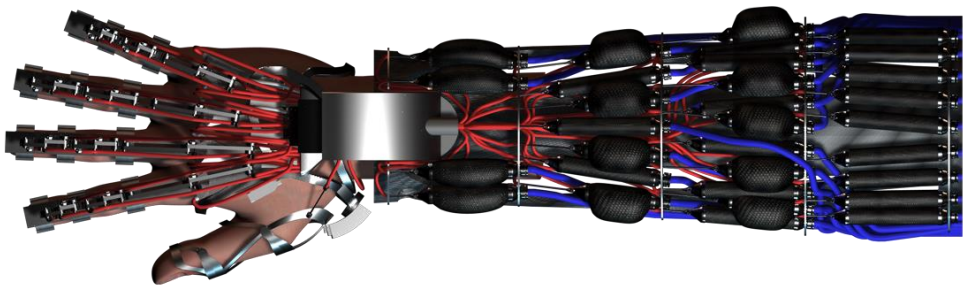

Fig 8.2: Top perspective of the rendered robotic glove

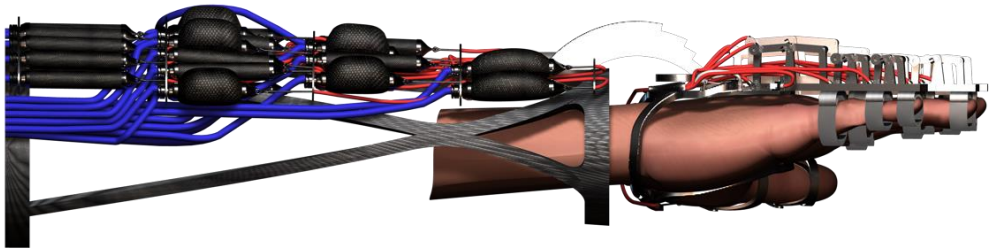

Fig 8.3: Right perspective of the rendered robotic glove

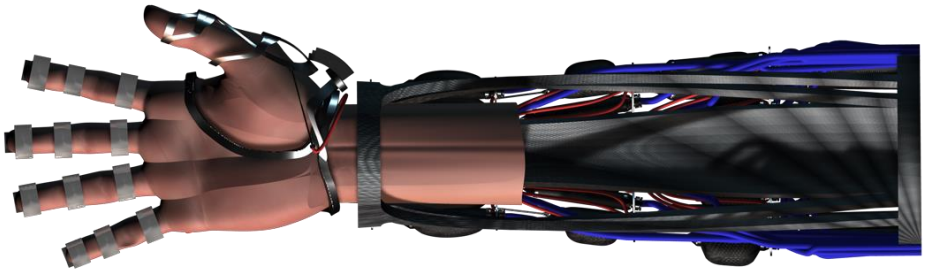

Fig 8.4: Bottom perspective of the rendered robotic glove

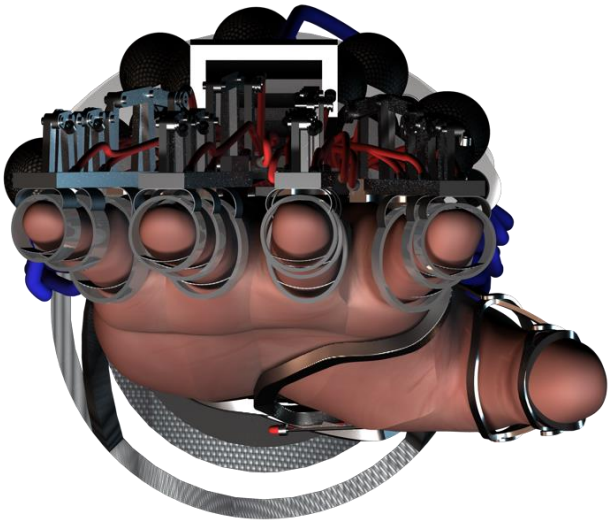

Fig 8.5: Front perspective of the rendered robotic glove

Fig 8.6: Back perspective of the rendered robotic glove